Digitone: A Novel Soccer Goalkeeping Device

A Major Qualifying Project Report:

Submitted to the Faculty

of the

WORCESTER POLYTECHNIC INSTITUTE

In partial fulfillment of the requirements for the

Degree of Bachelor of Science

By

David Polito

Tyler Wood

Joseph Rucco

Date:

Approved:

1. Soccer Goalkeeping Device
2. Finite Element Analysis
3. Biomechanics

Prof. Mark Norige, BME Advisor

Prof. Satya Shivkumar, ME Advisor

Abstract

Soccer goalkeeper hand injuries can be reduced with the use of a novel protective device modeled using computer aided design and evaluated with finite element analysis. A common thumb injury experienced by soccer goalkeepers is damage to the ulnar collateral ligament in the metacarpal phalangeal joint. Present devices and gloves lack adequate thumb protection from the high impact loading conditions experienced during game play. This report suggests that a device, printed in high strength polymer and analyzed using a physiologically accurate model of the thumb, will reduce injury. Additional work is needed to test a wearable glove version.

Table of Contents

Authorship

- Imaging research - Dave Polito, Tyler Wood
- Creation of solid bone meshes from CT scans – David Polito
- Creation of soft tissue in Abaqus™ – David Polito
- Research of mechanical properties for tissue – David Polito
- Simulations and data gathering for physiological model – David Polito
- SolidWorks™ Design – Joseph Rucco, Tyler Wood
- Simulations and data gathering for physiological model with device – David Polito, Tyler Wood
- Data interpretation – David Polito, Tyler Wood
- Validation of both models – David Polito
- Rapid prototyping – Tyler Wood, David Polito
- Commercialization Research –Joseph Rucco, Tyler Wood, David Polito
- Abstract – Tyler Wood, David Polito
- Executive Summary – David Polito
- Introduction – David Polito, Tyler Wood
- Literature Review – David Polito
- Project Strategy – David Polito, Joseph Rucco
- Alternative Designs – David Polito, Tyler Wood
- Design Verification – David Polito, Tyler Wood
- Discussion – David Polito
- Final Design and Validation – Tyler Wood
- Conclusion and Recommendations –David Polito, Tyler Wood

Acknowledgements

Our group would like to thank our WPI advisors, Mark Norige and Satya Shivkumar, for their guidance and support over the course of the project. We would also like to thank our off-campus advisor, Dr. Samandar Dowlatshahi, for bringing this project to the attention of the biomedical engineering department at Worcester Polytechnic Institute, as well as sharing his knowledge and experience with us. We are very grateful for the assistance of Dr. Ali Kiapour, who provided indispensable help and direction throughout the entire process of creating our model. Thanks are due to Adriana Hera for providing access to the Abaqus™ software and to Erica Stults for rapid prototyping. Finally, we want to thank the UMass Medical Radiology Department for the use of their MRI machine, as well as the National Institute of Health, who allowed us to access the hand CT images from their anonymous database.

Table of Figures

Table of Tables

Table of Equations

1 Introduction

Fine motor skills and manual dexterity in humans rely heavily on the thumb. As such, any injury sustained by this important digit can be devastating. This is particularly true for athletes, especially professional athletes whose livelihood depends on their ability to play a sport. In soccer, the goalkeeper must use his or her hands to prevent the ball from entering the goal at all costs. The development of protective gloves is a balance between increasing structural integrity while preserving the natural flexibility of the hand to allow for precise catching and parrying movements. Most products that exist on the market today incorporate protective dorsal spines. While this is effective in preventing hyperextension, it does not protect the thumb against excessive radial deviation, most commonly resulting in damage to the ulnar collateral ligament (UCL) of the metacarpal phalangeal joint (MPJ) of the thumb. Although damage to the radial collateral ligament (RCL) is also possible, UCL injuries are much more common; 60-90% of injuries to ligaments of the MPJ occur in the UCL (Patel).

The two mechanisms of injury to the UCL are acute trauma and chronic damage. These are referred to as Skier's Thumb and Gamekeeper's Thumb respectively (Cluett). Both injuries can affect a soccer goalkeeper, from either repeated forces exerted by the soccer ball during a catch or parry, or from a large trauma brought on by a fall or a particularly forceful shot. Treatment of this injury depends on multiple factors, such as extent of the injury, time elapsed since the injury, previous injury, and age (Cluett). If the tear is only partial, the patients thumb will be immobilized for approximately 4 to 6 weeks (Cluett). If the tear is complete, however, surgery is required to facilitate complete healing. The recovery time for this mechanism of injury is typically 3 to 4 months (Cluett).

The purpose of this project is to develop a method of preventing damage to the ulnar collateral ligament in soccer goalkeepers. The project team sought to create a device that can either be easily incorporated into the goalkeeper glove or worn separately from the glove without interfering with its

function. The device needs to provide protection without being overly complicated or cumbersome. In addition to preventing damage to the UCL, it should act to stabilize the entire MPJ in both abduction and extension.

In order to find an effective solution, the forces involved in injury must be thoroughly analyzed. Due to the nature of the high impact loading conditions involved in sports injuries, human testing is highly impractical. Using anatomical information and images from CT scans, a computer model of the metacarpal phalangeal thumb joint is constructed to gather data on the failure properties of the UCL. This data can be used to determine which part of the MPJ needs to be stabilized in order to prevent injury. With this data, a device design can be created using an informed engineering approach, rather than strictly empirical designs.

The background section outlines the mechanism of UCL injuries, anatomy of the thumb, and patents pertaining to hand protection in goalkeepers. The resulting device should prevent a common injury not resolved by existing products without compromising functionality. The project strategy gives in depth information about the objectives and constraints that were considered in the execution of our project. These objectives and constraints were also used to expand the initial client statement to a more concise and informative revised client statement that provides specific details on the capabilities final device should be able to do. The last section of the project strategy gives a brief overview of the general approach used in the project. The design alternatives section includes information about the needs that will be satisfied for this project, and expands upon the functions and specifications of the device with a feasibility study. Conceptual designs that were created empirically are listed in order and then compared with a function-means chart. The entire methodology used for the creation of the model of the MPJ is described in the design calculations section, and then preliminary data that validates the model is explored. The results of the MPJ model with the spine in place are detailed in design verification, and their meaning is explored in the discussion section. In addition, the impact of the device on several

different factors such as the environment, the economy, and society as a whole are discussed. The final design and validation describes the progression of designs and prototypes that lead to the final design of the spine. Finally, the conclusions drawn from the project and future recommendations are detailed.

2 Background

2.1 Injury Types

The most common injuries to the thumb are caused by hyperextension and excessive abduction. Hyperextension occurs when the thumb is bent backwards and the metacarpal phalangeal joint experiences excessive dorsal deviation (Dowlatshahi). This is a common injury in ball sports, particularly for a soccer goalkeeper. This injury can range from a sprain to a capsular tear, and as an extreme, dislocation of the dorsal joint (Dowlatshahi). A dorsal dislocation of the metacarpal-phalangeal joint is either labeled as simple or complex. When no soft tissue is torn, it is considered a simple dislocation. This can be treated without surgery (Dowlatshahi). A complex dislocation occurs when tissue is torn or a bony avulsion occurs, and requires reconstructive surgery (Dowlatshahi).

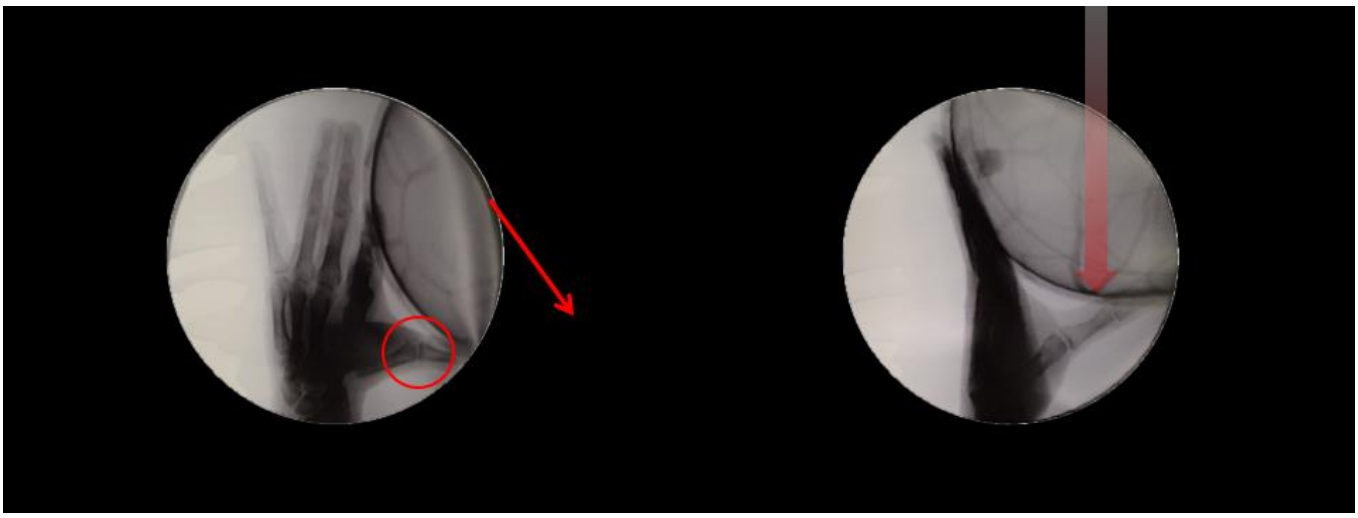

Figure 2-1: Lateral and Medial Injury of the MPJ (Dowlatshahi)

Abduction injuries are caused by excessive radial deviation about the metacarpal-phalangeal joint (Petre). Injuries to the ulnar collateral ligament are more common than injuries to the radial collateral ligament, with 60-90% of ligament injury occurring in the ulnar collateral ligament (Patel). There are two cases in which this occurs: with acute damage and with chronic damage. When the injury

is caused by chronic damage, it is referred to as Gamekeeper's thumb. This term was coined to describe an injury sustained by European gamekeepers, when the ulnar collateral ligament is stretched over time due to the repetitive wringing of the neck of game between the thumb and the forefinger (Dowlatshahi). When the injury is acute, it is referred to as Skier's thumb. It is named for the acute damage that can be suffered by a skier during a fall when the strap of the ski pole forcibly causes the thumb to deviate in a radial direction (Petre). Both injuries can occur in soccer goalkeepers, either from catching the ball over and over again, catching a shot with a particularly high velocity, or falling on the thumb. The thumb most commonly tears at the distal insertion site, but it can also tear mid-substance or at the proximal site (Petre). These tears can also be accompanied by a bony avulsion, which is an injury to the bone where the ligament attaches (Petre). This can be treated with surgery accompanied by suture anchors or by free tendon grafts (Petre).

2.2 Functional Anatomy

2.2.1 Bone and Joint locations

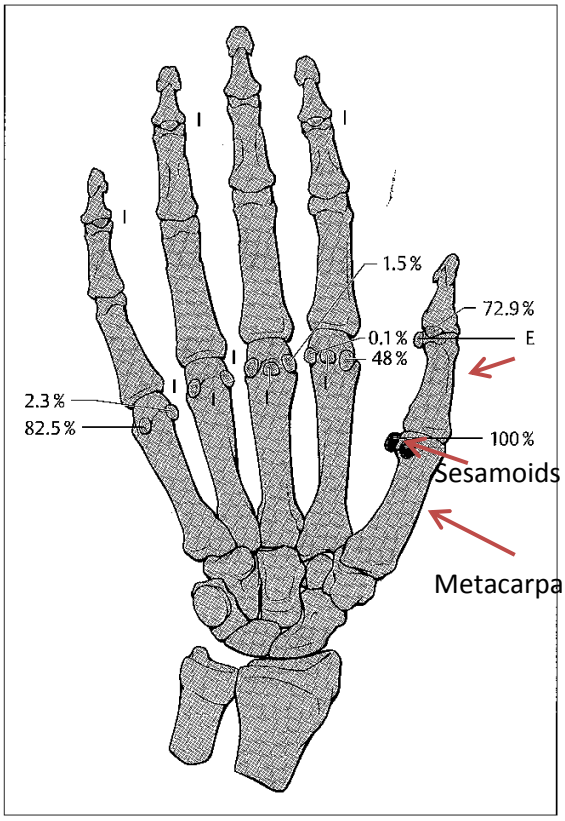

Figure 2-2: Location of Bones (Shmidt)

The thumb is composed of three principle bones: the metacarpal, the proximal phalanx, and the distal phalanx. The metacarpal is attached distally to a carpal bone in the wrist, and proximally to the proximal phalanx (Shmidt). The proximal phalanx is attached at the distal end to the distal phalanx (Shmidt). In addition to these three bones, there are two sesamoids that glide on palmar extensions of the distal articular surface of the metacarpal (Shmidt). The sesamoids are located between

the wall of the joint capsule and the palmar plate (Shmidt). The contact points of the bones result in three separate joints. The carpometacarpal joint results from the interaction of the carpal and the metacarpal. The metacarpal phalangeal joint results from the interaction of the metacarpal and the distal phalanx. The interphalangeal joint results from the interaction of the distal phalanx and the proximal phalanx.

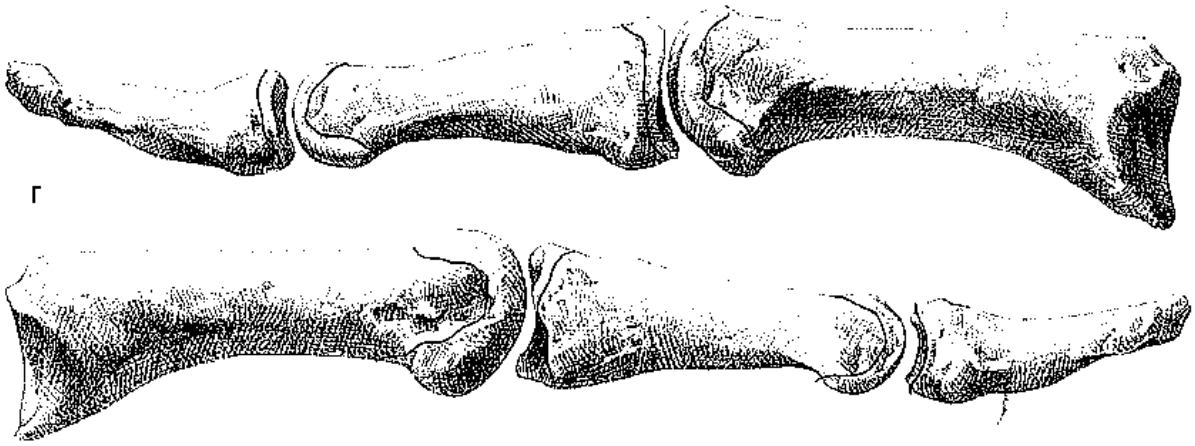

Figure 2-3: Radial and Ulnar View of the Bones of the Thumb (Shmidt)

2.2.2 Bone Composition

On a macroscopic level, bone is composed of two types: cortical, also known as compact bone, and cancellous, or trabecular bone. These bone types work in tandem to provide the body with skeletal support. Cancellous bone has a high surface area, but compared to cortical bone, it is less dense and has a significantly lower elastic modulus. The primary functional unit of cancellous bone, the trabecula, is composed of collagen and allows the bone to resist tension. Cancellous bone is also the site of red blood cell production. Cortical bone is denser and has an elastic modulus orders of magnitude greater than cancellous bone. Cortical bone protects internal organs, supports the body, and allows for normal movement.

2.2.3 Muscles

There are seven muscles that act on the MPJ of the thumb (Smutz). The four extrinsic muscles are the extensor pollicis brevis (EPB), the flexor pollicis longus (FPL), the extensor pollicis longus (EPL), and the abductor pollicis longus (APL) (Smutz). The three intrinsic muscles are the flexor pollicis brevis (FPB), the abductor pollicis brevis (APB), and the extensor pollicis longus (EPL) (Smutz). The adductor pollicis can be regarded as the combination of an oblique (ADPo) and transverse (ADPt) head (Smutz). Together, these muscles exert forces that stabilize the individual joints of the thumb (Shmidt). In the MPJ, the FPL, FPB, ADPt, and ADPo are the major flexors, with the FPL contributing the most (Smutz). The APB is a mild flexor of the MPJ (Smutz). In extension, the EPL and EPB are the only contributing muscles, with the EPL contributing the most (Smutz). The APB , FPB, and EPB contribute to abduction, with the APB contributing the most (Smutz). The EPL, ADPt, and ADPo are the major adductors (Smutz). The FPL does not contribute significantly to either adduction or abduction (Smutz).

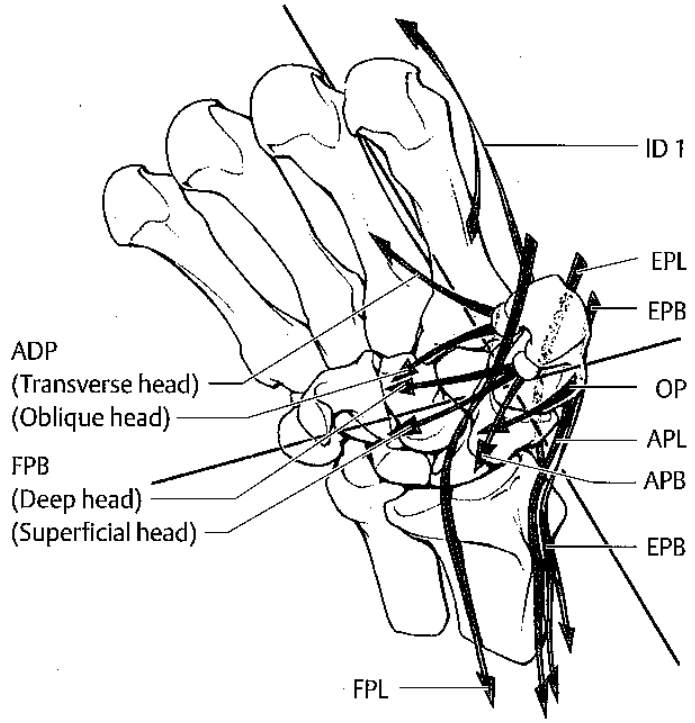

Figure 2-4: Directional Effects of Intrinsic and Extrinsic Muscles (Shmidt)

2.2.4 Tendons

There are three main tendons that influence the thumb (Shmidt). The tendon sheath of the flexor pollicis longus passes through the carpal tunnel and inserts into the distal phalanx (Shmidt). It is reinforced by the A1 and A2 pulleys (Shmidt). A complex of reinforcing fibrous structures extends in between the A1 and A2 pulleys. It is further divided into a proximal annular portion and a distal oblique portion (Shmidt). The annular portion originates from the insertion fibers of the adductor pollicis muscle and the proximal ulnar portion of the proximal phalanx (Shmidt). The oblique portion runs distally from the annular portion and attaches to the radial part of the interphalangeal joint, where it fuses with the joint capsule and the palmar plate (Shmidt). The extensor pollicis longus extends obliquely through the middle of the MPJ and past the proximal phalanx, where it inserts into the base of the distal phalanx (Shmidt). In the MPJ, it is contained under a hood formed by the inserting tendons of the short muscles in the thumb (Shmidt). The extensor pollicis brevis travels through the middle of the MPJ and inserts into the proximal portion of the proximal phalanx (Shmidt). All three of these tendons allow the MPJ of the thumb to both flex and extend (Shmidt). The tendons of the MPJ are composed of dense fibrocartilage, which is made of types I and III collagen (Petre).

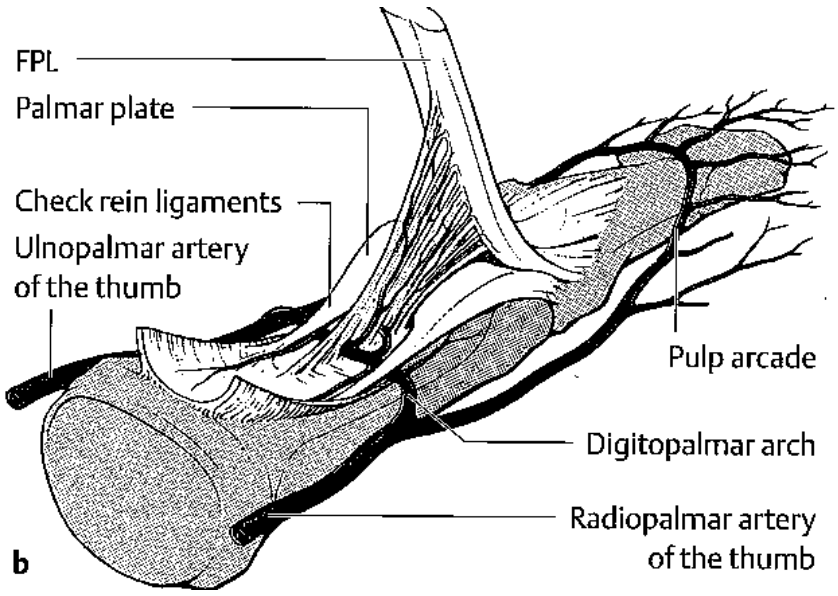

Figure 2-5: Distribution of the Flexor Pollicis Longus (Shmidt)

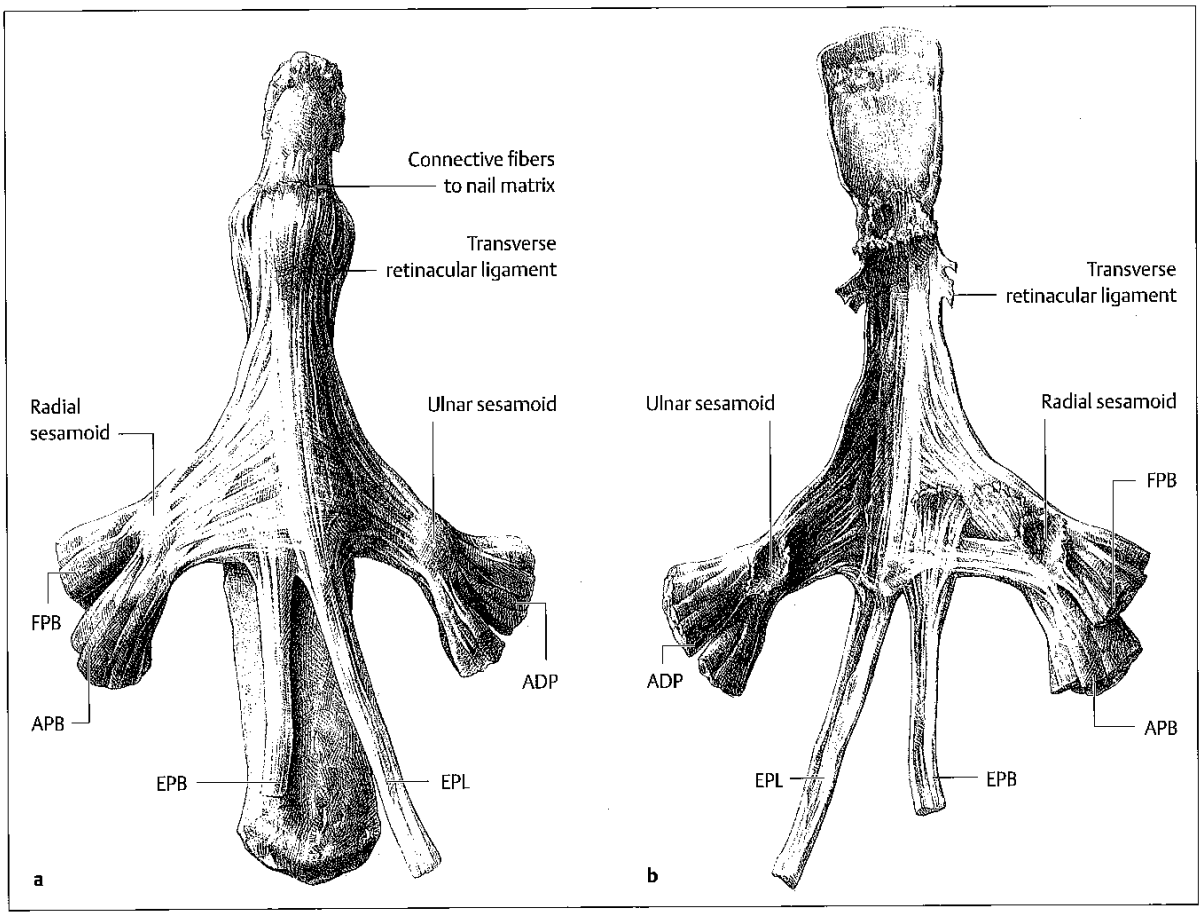

Figure 2-6: Dorsal Aponeurosis of the Thumb (Shmidt)

ADP - adductor pollicis

2.2.5 Joint Capsule

Stabilization of the MPJ comes from the joint capsule, which is reinforced by several ligaments, as well as the volar and palmar plate (Petre). It attaches around the circumference of the joint (Petre). It is filled with synovial fluid that lubricates the articular cartilage on the ends of the bones (Petre). The most superficial ligaments are the radial and ulnar phalangoglenoidal ligaments (Shmidt). They are attached at the base of the proximal phalanx on one end and to their respective sesamoid on the other (Shmidt). The MPJ capsule also possesses radial and ulnar collateral ligaments. These ligaments provide lateral and dorsal stability for the proximal phalanx. The UCL originates from the dorsal ulnar portion of

the metacarpal head and attaches to the medial tubercle of the proximal phalanx (Shmidt). The RCL originates from the dorsoradial portion of the metacarpal head and attaches to the lateral tubercle of the proximal phalanx (Shmidt). Each collateral ligament is made of two other ligaments: the proper ligament, which is larger of the two, and the accessory ligament (Petre). The accessory ligaments are shaped like fans, and insert into their respective sesamoids (Shmidt). The sesamoids are further restrained by the adductor pollicis tendon on the ulnar side and the flexor pollicis brevis tendon on the radial side, as well as the A1 pulley, which runs laterally across the palmar side of the proximal phalanx and attaches at both the palmar plate and the base of the proximal phalanx (Shmidt). The proper ligament attaches between the metacarpal head and the base of the proximal phalanx (Petre). The palmar plate is a special thickening of the joint capsule (Petre). It rests directly on the palmar side of the joint and extends from the proximal phalanx to the metacarpal (Shmidt). It is attached both radially and laterally by two check rein ligaments (Shmidt). The plate also helps to prevent hyperextension in the digits. During flexion, the check rein ligaments fold into the space under the metacarpal; during extension, they become taut and help provide resistance against hyperextension (Petre). The volar plate is a specialized segment of the joint capsule (Petre). It helps seal the joint as well as to stabilize it. Both the palmar and volar plates are made up of dense, fibrous connective tissue lined by synovial tissues.

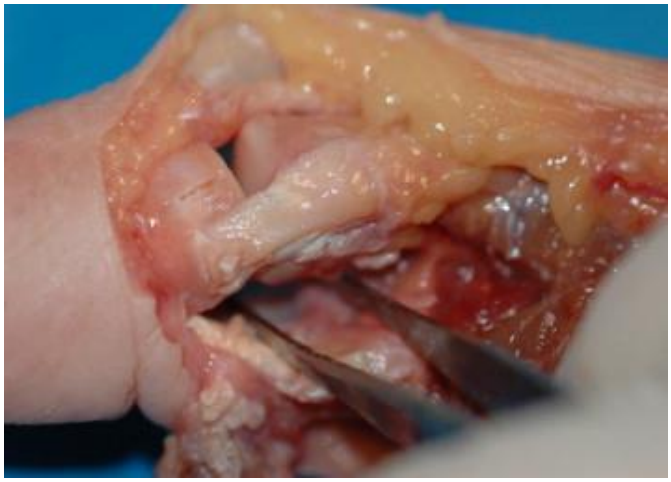

Figure 2-7: Surgical View of the ulnar collateral ligament (Carlson)

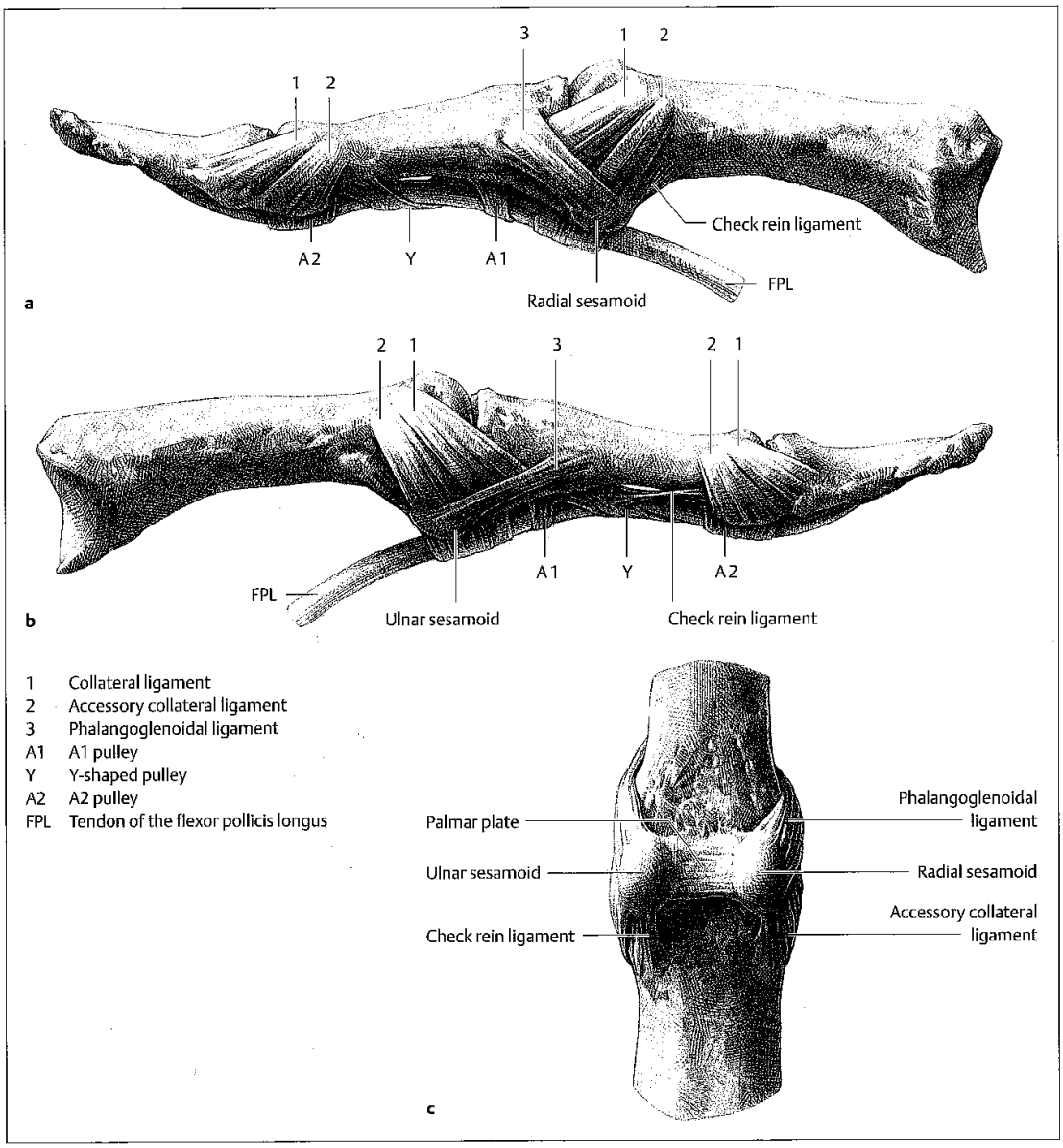

Figure 2-8 Capsular Ligaments of the MPJ (Shmidt)

2.2.6 Hyaline Cartilage

Cartilage can be divided into three different categories: hyaline, elastic, and fibrocartilage. Hyaline cartilage, often referred to as articular cartilage, is by far the most prevalent in the body, serving to reduce friction in joints and provide structure in early stages of human development (Roughley). Hyaline cartilage is characterized by a high content of proteoglycan aggrecan (Roughley). Together with hyaluronan and link proteins, it forms proteoglycan aggregates (Roughley). These aggregates give hyaline cartilage its turgid nature, as well as the ability to resist compressive forces in articular cartilage due the osmotic properties it imparts (Roughley).

2.2.7 Fibrocartilage

Fibrocartilagenous material is most notably found in the menisci of the knee and the discs of the temporomandibular joint, although it is also makes up the joint capsule and plates of the MPJ (Benjamin). Unlike hyaline cartilage, it lacks a perichondrium, which assists in the growth and repair of cartilage (Benjamin). Its structural and functional properties lie between hyaline cartilage and dense fibrous connective tissue (Benjamin). The majority of cells that comprise the fibrocartilage resemble chondrocytes and fibroblasts, although it is often difficult to differentiate between them (Benjamin). In general, chondrocytes compose the center and fibroblasts the outer layers (Benjamin). The collagen fibers in the fibrocartilage can be arranged in several conformations, but in the plates of the MPJ it resembles a basket woven pattern (Benjamin). This particular type of cartilage is reported to function as a resistor of shear and compressive forces (Benjamin).

2.3 Applications in Soccer

Soccer goalkeepers are constantly at risk for painful and debilitating hand injuries. For over 70 years, hand protection was not available to goalkeepers even though the first patent was filed in 1885 by William Sykes (Grahame). Amadeo Carrizo is reported to be the first goalkeeper to wear gloves, playing in the late 1940s (Grahame). In the 1970s, goalkeeper gloves became more popular, appealing to both amateur and professional players. Sepp Maier worked in tandem with Reusch® to design the soft grip glove, which would eventually become the basis of the modern goalkeeping glove (Grahame). In the 1990s, companies began to become more aware of the market potential of a goalkeeping glove. Multiple types of gloves were designed for different variable situations, such as location and weather. Companies today are focusing more and more on digit and wrist protection.

2.4 Current Products and Patents

2.4.1 Patents

Several patents were awarded to designs claimed to prevent thumb injury and hyperextension. Two of the patents immobilized the thumb and the metacarpal phalangeal joint in several directions to help alleviate the threat of injury (Appendix D, Appendix E). This immobilization is not ideal for a goalkeeper as they must control the ball and direct throws or catch the ball during the course of a game. Other patents use a second layer of padding to prevent injury, but this is not useful in the case of abduction (Appendix F). There is a patent that utilizes a gusset between the thumb and pointer finger (Hochmuth). This gusset is not designed to prevent injury, merely to increase the surface area of the glove.

2.4.2 Market Standard

The gold market standard for finger protection right now is dorsal spines. These spines allow for full mobility in flexion of the fingers, but prevent hyperextension. These spines are currently only utilized on the 2^{nd}-5^{th} digit, and not the thumb. Despite the effectiveness of some of these devices, there are currently no devices that are designed for a goalkeeper that can prevent injuries to the metacarpal phalangeal joint while still allowing enough mobility for effective play during a soccer match.

3 Project Strategy

3.1 Initial Client Statement

As previously stated, fine motor skills rely heavily on the thumb. Any damage sustained by the thumb can inhibit an individual's ability to perform basic hand functions such as grabbing, holding, and gripping. In ball sports, thumb injuries are fairly common. Damage can be particularly debilitating for athletes who rely on their hands, such as soccer goalkeepers. When a goalkeeper catches a ball, there is an impact force. Depending on what part of the hand is affected, it can cause hyperextension and abduction injuries at the metacarpal phalangeal joint. The abduction injuries can be acute, referred to as Skier's thumb, or chronic, referred to as Gamekeeper's thumb. There are currently no patents or products found by the team addressing the damage that can be caused by over-abduction of the thumb at the MPJ. In order to combat this injury, a novel soccer goalkeeping device is being proposed. The initial client statement is as follows:

> *To design a novel soccer goalkeeping glove that prevents injury from both abduction and extension of the thumb.*

3.2 Objectives

Objectives describe what a device should be. In this section, objectives for the device will be stated and described. These objectives were created by the project team through a series of brainstorming sessions and qualitative analysis of previous devices.

The device should be effective. This refers to its ability to perform all of its functions consistently and without fail. It should be both durable and reliable. In terms of durability, the device should be able to be used repeatedly without sustaining any damage or impeding its functions. With respect to

reliability, it should be able to perform its functions consistently and without fail. These two objectives combined will result in a device that is effective.

The device should also be marketable. Without marketability, the device will not sell, and therefore will be pointless in its design. The device needs to be cost efficient, which means that the cost of materials should be low and it should be easy to manufacture in mass quantity. The device should also be innovative. It cannot infringe on any current patents, and it must be a new design in order to appeal to customers. It should also be aesthetically pleasing, again to appeal to customers. The device must also come in multiple sizes to accommodate for different goalkeepers.

The device should also be easy to use. It should be at least as comfortable as current glove designs so goalkeepers will want to use it. It should also be as flexible as gloves that are currently on the market. The glove should match any competing glove for ease of use in order for it to be a viable choice for goalkeepers when selecting a glove.

The objectives tree in Appendix I shows how the objectives relate to one another. At the top of the tree is the device itself. The next tier of objectives includes effectiveness, marketability, and ease of use. These objectives are further divided into another tier. The effective objective includes reliability and durability. Marketability includes cost, innovation, aesthetics, and varying size. Cost is further divided into cost of materials and cost of manufacturing. Ease of use includes comfort and flexibility. In addition, the pairwise comparison chart in Appendix J shows a numerical comparison of the objectives.

3.3 Constraints

Constraints describe the restrictions or limitations relevant to the device. In this section, constraints for the device will be stated and described.

The device cannot allow for more than 10 degrees in extension, 50 degrees in flexion, and 10 degrees in adduction/abduction in the MPJ. These numbers describe the normal movement of the metacarpal phalangeal joint (Dowlatshahi). When these are exceeded, there is a chance for injury.

There are two constraints in regards to cost. The project team was allocated 346 dollars. This money will be used to create a prototype and a mechanism to test it. For the final design, the device should not have a manufacturing cost of more than 25 dollars, because the device itself should only constitute a small part of the manufacturing cost of the complete glove.

Time is another constraint of this project. The design must be finished in one academic year. This is the amount of time to design, test, and create a prototype, as well as compile a report. Ideally, this should be done before the end of the academic year, so the time allotted is approximately 24 weeks.

The device must be effective on both hands. Goalkeepers wear gloves on both hands, so the mechanism that prevents injury must be able to function in both a left handed glove and a right handed glove.

3.4 Revised Client Statement

The initial client statement is vague in the sense that it only states that injury must be prevented. This only states one of the functions of the device. It does not address any of the objectives or constraints that were stated previously. In order to rectify this, a new client statement was written.

> *The objective of this project is to design, create, and test a novel device for soccer goalkeepers. The device should prevent injury from abduction/adduction and hyperextension of more than 10 degrees of the metacarpal phalangeal joint. The device can either be a new design or a modification of current goalkeeping gloves and/or devices. The device will either need to match or exceed the comfort, control, and range of hand mobility of current gold market standard goalkeeping gloves. The design must be durable enough to withstand the standard wear and tear associated with the activities of a goalkeeper. The cost of manufacturing the device must allow for a retail cost that will be competitive. The device must be safe for the goalkeeper to use. It must be able to withstand 700 Newtons of impact force. It should be marketable, in that it has a reasonable cost, is innovative, is aesthetically pleasing, and varies in size so all goalkeepers will be able to use it.*

This new client statement is much more informative than the previous one. It describes at what degree of extension and abduction injury can occur, as well as how much impact force it needs to be able to withstand. It also addresses all of the objectives that are laid out in the next section.

3.5 Project Approach

The goal of the project is to create a novel goalkeeper device that will protect the metacarpal phalangeal joint from hyperextension and excessive abduction. This device will need to surpass the current ratings of protection of the gloves used on the pitch today.

First, a testing method for the device will need to be developed. A test method that involves applying high impact forces to human thumbs is unreasonable, so a finite element model will be created and analyzed. The finished model will then be used in simulations, where it will be subjected to the impact force of a professionally kicked soccer ball in multiple directions.

After the results of the tests have been analyzed, it will be clear which areas of the metacarpal phalangeal joint require the most protection. This data will be used to create a novel device design to protect the metacarpal phalangeal joint. The design will need to protect against hyperextension and abduction. However, it will also need to allow the same amount or better mobility qualities than the current models of goalkeeping gloves.

The novel device must then be tested in order to calculate is values of protection. It will be modeled and assigned material properties using the proprietary software Solidworks™ and Abaqus™. The model of the device will be added to the previously constructed thumb model, and subjected to the same simulation tests. The data will show that the device reduces the forces experienced by the metacarpal phalangeal joint in both abduction and hyperextension. It will also relieve stress placed on the ulnar collateral ligament. This novel device will allow for the mobility of current devices while offering more protection to the thumb and the metacarpal phalangeal joint.

4 Design Alternatives

4.1 Needs Analysis

Current finger protection used in goalkeeping gloves are not utilized in the thumb. They are only placed in the other four digits; in addition, their main function is to prevent hyperextension, and does not take into account the effects of excessive abduction. The material that the gloves are made of provides some support, but not enough to prevent injury at very high forces. The need that the device developed through this project will satisfy is the successful prevention of injury to the UCL under high-impact loading conditions.

4.2 Functions and Specifications

The purpose of this device is to prevent injury to the thumb from both over-abduction and hyperextension. In order to achieve this goal, certain functions and specifications must be met. Functions describe what the device will do, and specifications describe how the functions will be met.

The first function is to prevent over-abduction of the metacarpal phalangeal joint. In doing so, Skier's thumb induced by acute damage and Gamekeeper's thumb induced by chronic damage can be avoided. In order to accurately describe how over-abduction will be prevented, a range of motion for the metacarpal phalangeal joint in abduction must be investigated. The range of abduction differs depending on the amount of flexion experienced by the metacarpal phalangeal joint. In the neutral position, i.e. at 0^o extension, the mean abduction of the right thumb is 19^o and the mean abduction of the left thumb is 21^o (Malik). At 30^o flexion, the mean abduction of the right thumb is 29^o and the mean abduction of the left thumb is 31^o (Malik). Based on these values, it was decided that the metacarpal phalangeal joint should not be allowed to abduct more than 15^o.

The device must allow for normal hand mobility. In order for a soccer goalkeeper to perform effectively, full range of motion must be allowed. Since the device will be affecting only the metacarpal phalangeal joint, range of motion must be established. In the metacarpal phalangeal joint, total range of motion was measured at 55° to 176°, with a mean of 110° (Yoshida). This range of motion varies based on the shape of the metacarpal head (Yoshida). Based on these figures, a range of motion of 160° should be allowed in the metacarpal phalangeal joint.

4.3 Feasibility Study

The largest difficulty of this project was creating an effective test method. Since this project involves creating a device that prevents injury in the thumb, using human subjects would be hazardous and unethical. It would also be unreasonable to use cadaveric subjects as well, due to a difficulty in obtaining test subjects and the likelihood of inaccurate result. It was determined that the best testing method would be to create a finite element model of the MPJ. This was achieved using the finite element analysis software Abaqus™. The difficulty of this approach was the project team's unfamiliarity with finite element analysis coupled with the complexity of the model. It took a significant amount of time to create the model, which limited the amount of detail that could be included.

4.4 Conceptual Designs

4.4.1 Long Spine

The long spine design incorporates a long plastic spine into the backing of the thumb as well as elastic bands that keep it tight and secure. The spine will include flex grooves that will allow it to bend with natural motion of the thumb. When the thumb begins to hyperextend, the spine stiffens to prevent further motion. In the lateral direction, the curvature of the spine prevents over-abduction of the metacarpal phalangeal joint and therefore prevents the rupture of the ulnar collateral ligament. This is achieved by the elastic bands that hold the spine tightly to the thumb and prevent unwanted motion.

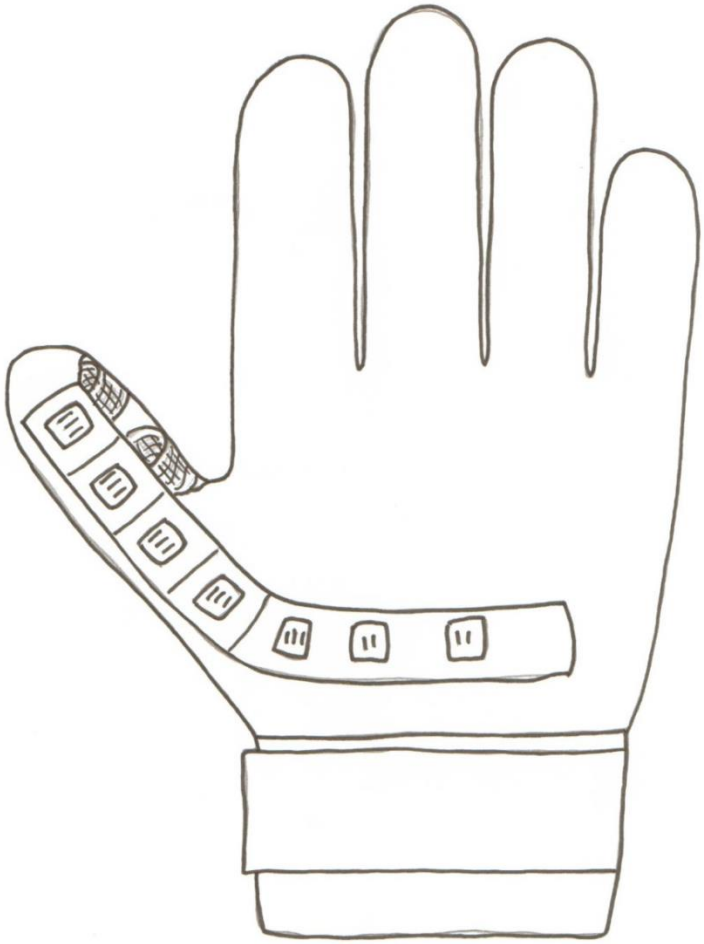

Figure 4-1: Long Spine

4.4.2 Casing/Backing

The casing or backing design prevents the most movement of all the alternative designs. The plastic backing runs along the back of the hand and wraps slightly around both the distal and proximal sides of the hand. This allows for a secure fit on the hand and the thumb. Because the casing wraps around the thumb, this prevents movement of both hyperextension and over abduction. The design also includes connected pieces on the thumb that allow for it to bend.

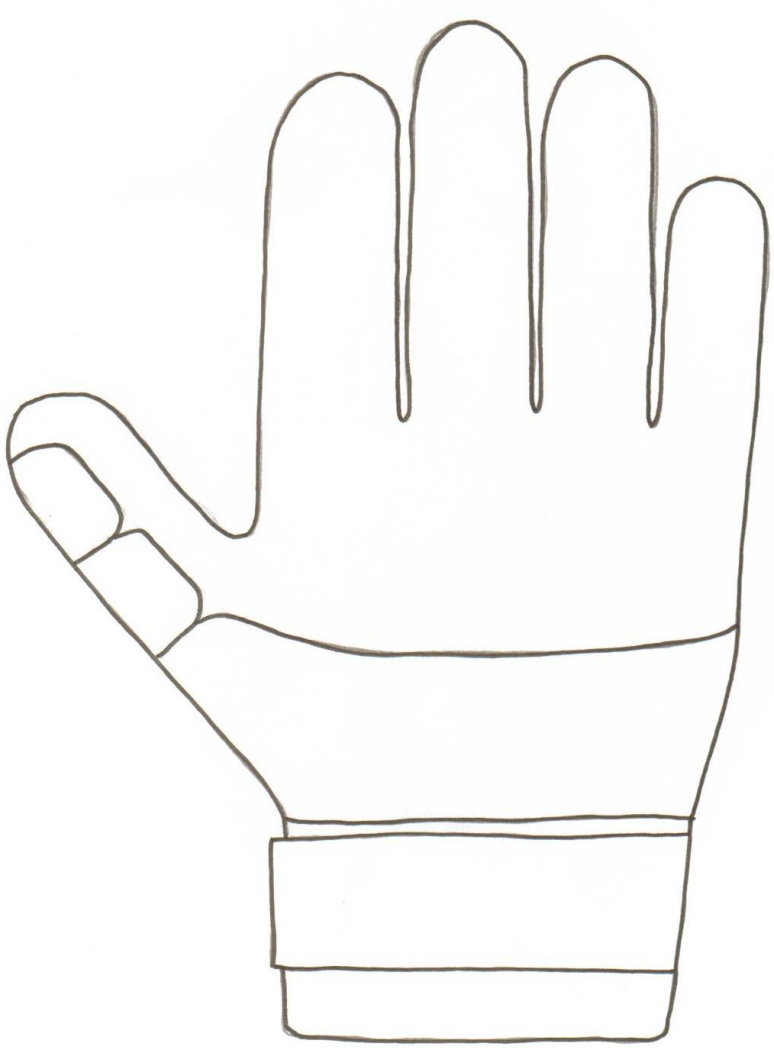

Figure 4-2 Casing/Backing

4.4.3 Gusset

This design uses two components to achieve the desired result. The first is a short spine on the back of the thumb. This spine will stiffen when a force is applied to it that extends the thumb. It acts much like the spine in the Long Spine design in that it prevents hyperextension. However, this design also utilizes a gusset that connects the first and second digit of the hand. The gusset will be made of an elastic material that allows for some stretch but after a certain force has been applied will stiffen and prevent any further motion. This would not allow for the thumb to over abduct in the later direction.

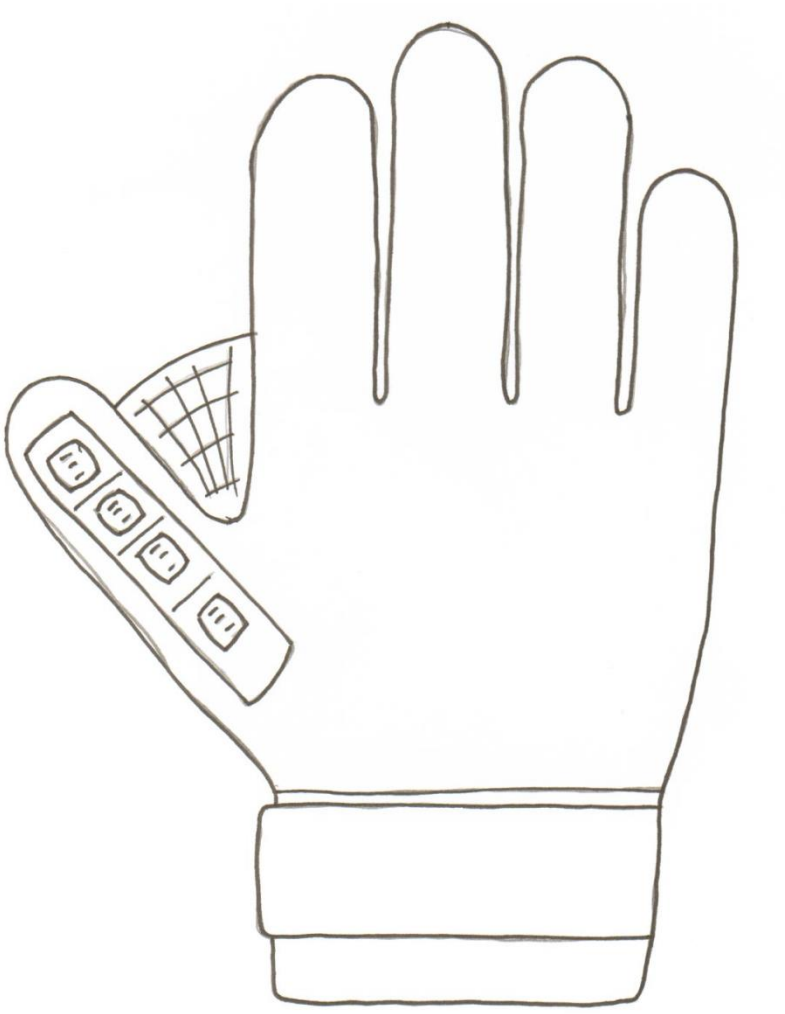

Figure 4-3: Gusset

4.4.4 Elastic Wrapping

The elastic wrapping design is completely separate from the glove and could be worn on its own if the user desired. The wrap consists of an elastic material much like that of an ACE™ Bandage. It would provide compression to the metacarpal phalangeal joint and this compression would help to alleviate unwanted movement due to the forces that act on thumb.

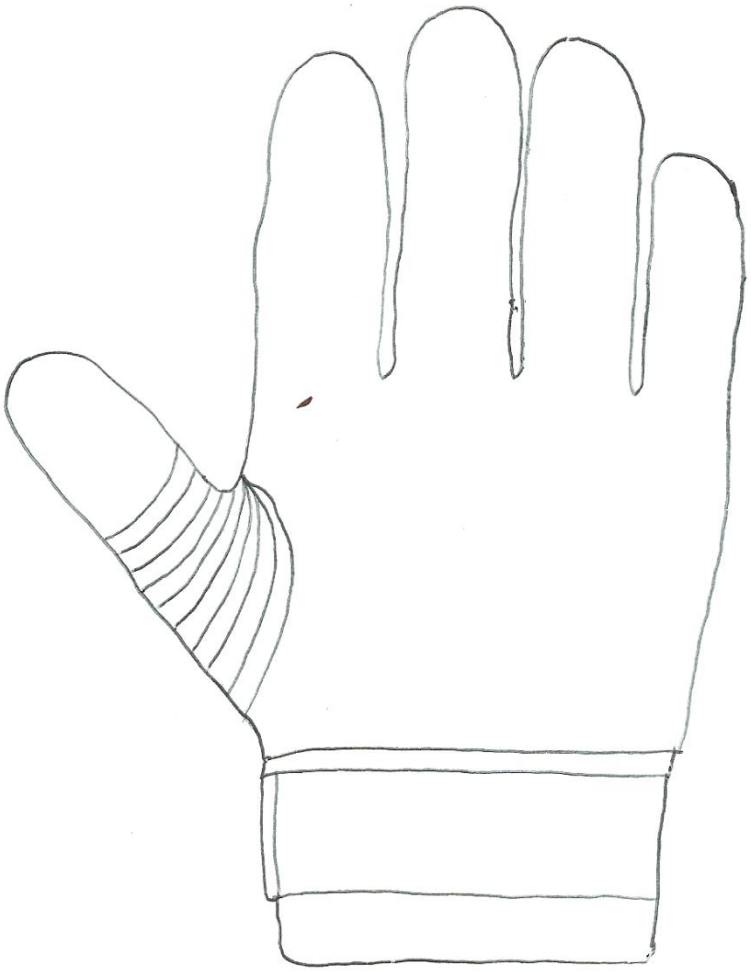

Figure 4-4: Elastic Wrapping

4.4.5 Vertebrae

The vertebrae design incorporates several interlocking pieces to prevent unwanted movement of the thumb. When a force is applied to the thumb that causes it to extend or abduct, the pieces lock together and prevent the movement. The design acts very similarly to a spine; however, the vertebrae wrap around and enclose the thumb to also provide further impact protection.

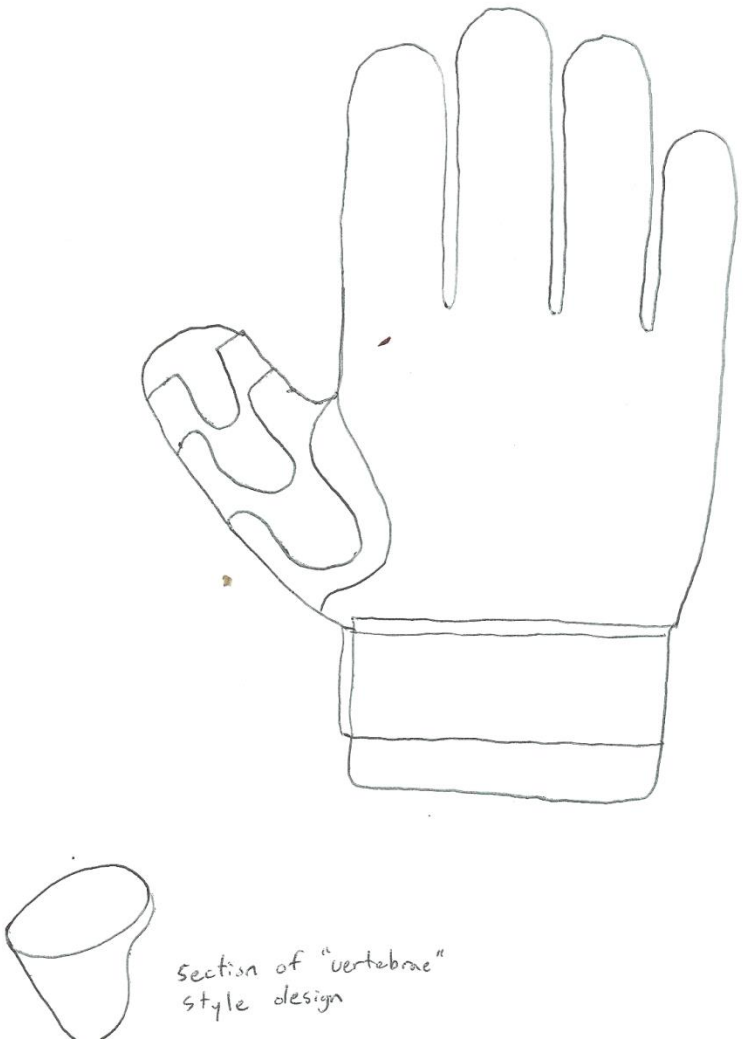

Figure 4-5: Vertebrae

4.4.6 Plates

In this design anatomically placed plates are used in order to prevent unwanted movement. The plates will be positioned in order to allow for the natural movement of the thumb in bending and flexion. When the thumb begins to hyperextend or over-abduct, the plates will meet and prevent motion that could induce injury. This design allows for a large amount of mobility while still incorporating good protection from common forces.

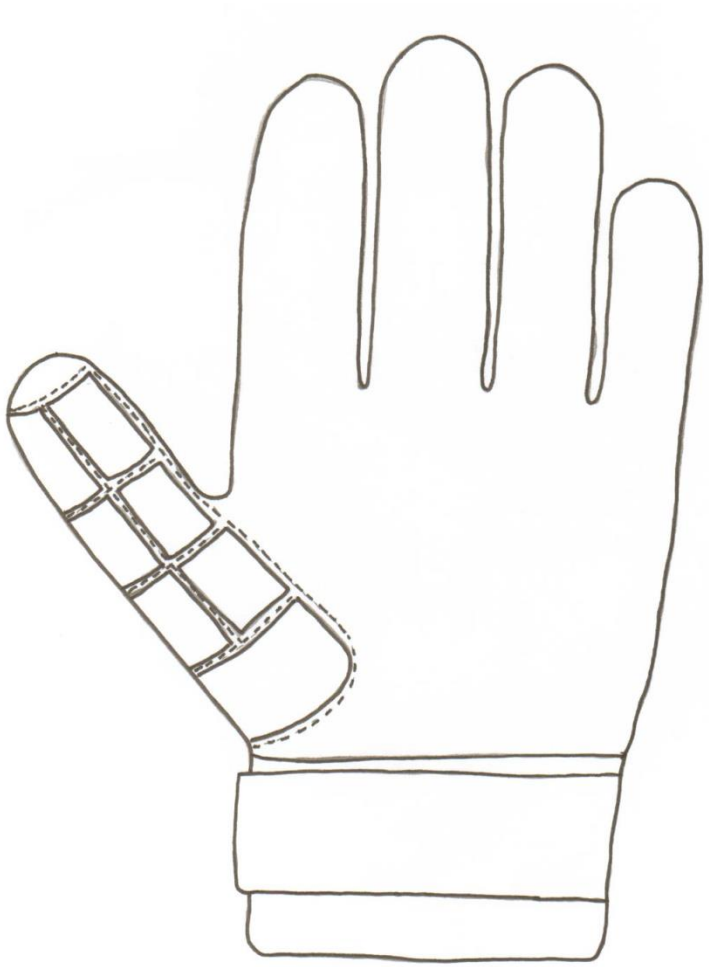

Figure 4-6: Plates

The six designs were placed into a function-means chart for qualitative analysis. Due to time constraints, the project team was unable to model all of them using Solidworks™ and Abaqus™ to quantitatively analyze their efficacy. The function-means charts are shown in Table 4-1 and Table 4-2.

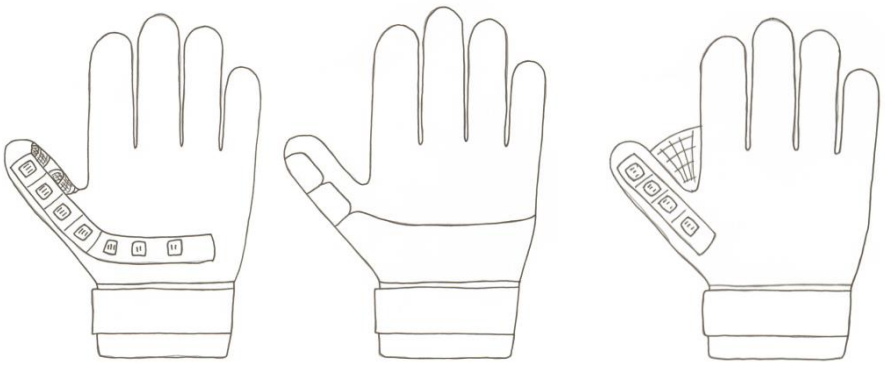

	Means		
Function	Long Spine	Back Brace	Gusset/Spine
Prevent Hyperextension of MP Joint	Long spine prohibits hyper extension	Plastic backing does not allow for the thumb to hyper extend	Small spine prohibits hyper extension
Prevent Over Abduction of MP Joint	Curvature of spine and elastic bands help to lock thumb in place and prevent abduction	The backing curves around the thumb to prevent abduction	Gusset elastic between thumb and forefinger does not allow for over abduction
Allow Normal Mobility	Flex grooves in spine allow for normal thumb bending	Slits in backing on the thumb joints allow for the thumb to bend	Flex grooves on spine allow for thumb bending, adduction of thumb is unrestricted by gusset

Table 4-1: Function-Means Chart Part 1

	Means		
Function	Elastic	Vertebrae	Squares
Prevent Hyperextension of MP Joint	Provides compression to lower thumb to minimize displacement	Uses interlocking sections of sturdy material to restrict the thumb's movement to a safe range of motion	Square pieces meet and prevent further movement during extension
Prevent Over Abduction of MP Joint	Provides compression to lower thumb to minimize displacement	Uses interlocking sections of sturdy material to restrict the thumb's movement to a safe range of motion	Square pieces meet and prevent further movement during abduction
Allow Normal Mobility	Reinforces thumb but does not restrict movement	Restricts the thumb's movement in unsafe ranges while providing minimal restriction in the normal range of motion	Squares do not meet during normal hand movements

Table 4-2: Function-Means Chart Part 2

Although the function-means chart seems to show that all the designs can provide the necessary functions, it was determined that the back brace would restrict normal movement too much to be effective. In addition, the squares and elastic would not provide enough support to prevent injury. The gusset design would most likely provide enough support, but it may interfere with the goalkeeper's ability to catch the ball at certain angles. The vertebrae and long spine designs were chosen as the most likely candidates to meet all the functions.

4.5 Design Calculations

This section describes the entire process of creating the model system that we used to test the efficacy of our device.

4.5.1 The Model System

This model of the MPJ consists of the tissues shown in Table 4-3.

Hard Tissue	Phalangeal Bone	Metacarpal
		Proximal Phalanx
	Sesamoid Bones	Ulnar Sesamoid
		Radial Sesamoid
Soft Tissue	Hyaline Cartilage	Metacarpal Cartilage
		Proximal Phalanx Cartilage
	Fibrocartilage	Palmar Plate
		Volar Plate
	Ligaments	Accessory Ulnar Collateral Ligament
		Proper Ulnar Collateral Ligament
		Ulnar Phalangoglenoidal Ligament
		Ulnar Check Rein Ligament
		Accessory Radial Collateral Ligament
		Proper Radial Collateral Ligament
		Radial Phalangoglenoidal Ligament
		Radial Check Rein Ligament

Table 4-3: Tissues Included in Evaluation Model

4.5.2 Modeling the Bone

In order to create an accurate model of the MPJ, the metacarpal and proximal phalanx bone must be modeled. MRI images were obtained courtesy of the radiology department at UMass Medical in Worcester, MA. The files were obtained as file type DICOM, which is a data format created by the Digital Imaging and Communications in Medicine and is currently the standard for medical image processing

and distribution. Scans of the base of the metacarpal to the end of the distal phalanx were obtained with a slice thickness of 0.5mm and a pixel size of 0.39mm. David Polito, Tyler Wood, and Samandar Dowlatshahi all had their right hands scanned. Unfortunately, these scans were insufficient for accurately creating a 3D model, and different physiological images had to be obtained. The comparison of the two can be seen in Figure 4-7. The MRI image on the left is grainy, compared to the CT image on the right which is clearly defined.

CT scans of the forearm and hand were obtained from the NIH database. The images have a slice thickness of 0.5mm and a pixel size of 0.25mm. These images are superior in contrast and resolution to the MRI scans previously obtained. In addition, CT scans are best utilized for identifying bone structures, which is ideal for creating solid bone models.

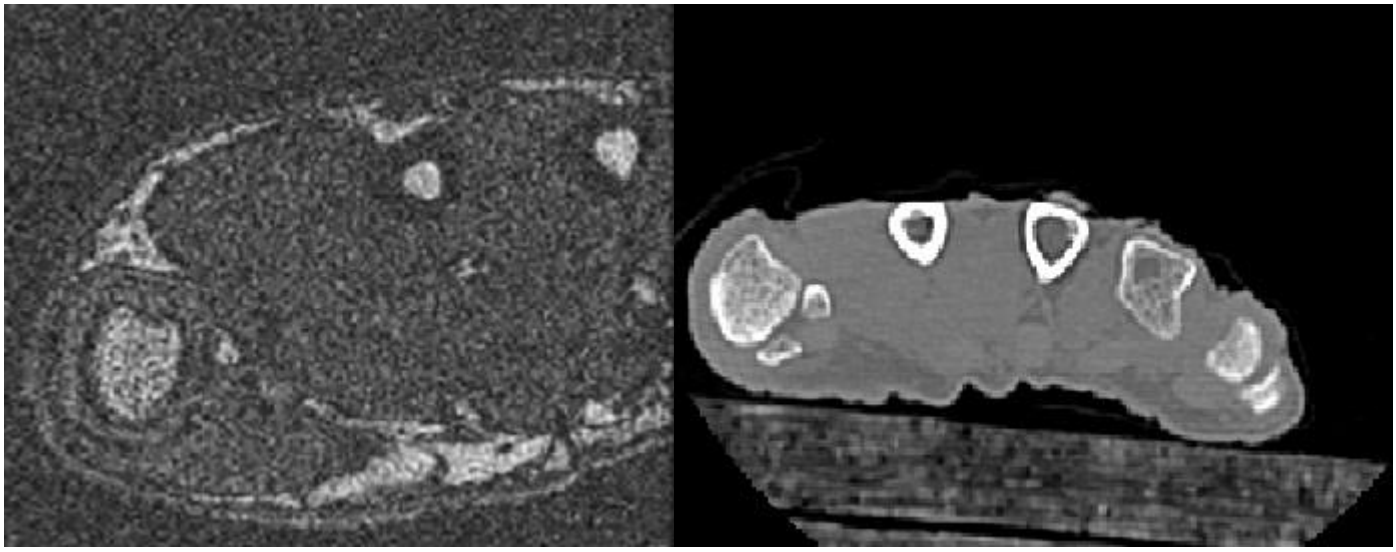

Figure 4-7: Comparison of the Quality of the MRI and CT Scans

Using a combination of 3D Slicer™ 4.2.1 and DeVIDE™ 12.2.7, surface models of the bones were created. The software isolates certain pixels based on their coloring and relation to each other.

To create a solid mesh, the surface model files were imported into IA-FEMesh™. Using this software, blocks that define the meshing points were created and assigned. The surface models were

then meshed and exported as input (.inp) files for use with Abaqus™. The mesh of the metacarpal consists of 36,960 separate elements, the proximal phalanx mesh consists of 12,870 separate elements, the ulnar sesamoid mesh consists of 2,912 separate elements, and the radial sesamoid mesh consists of 2,352 separate elements. The input file created from the four bones was imported into Abaqus™ and combined to create a model with accurate bone placement. The surfaces, blocks, and meshes of the metacarpal and both sesamoids can be found in appendices B and C.

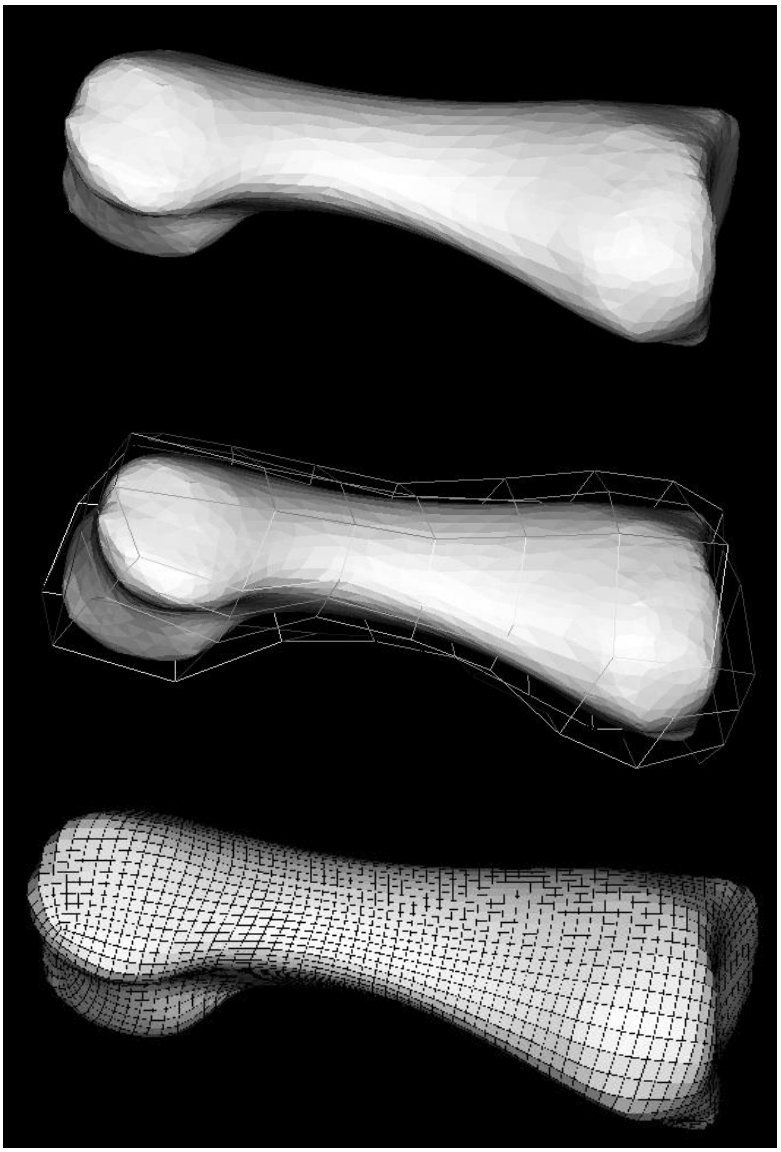

Figure 4-8: Surface, Block, and Mesh of the Proximal Phalanx

4.5.3 Modeling the Soft Tissue

Soft tissues could not be obtained from the MRI or CT images, so they had to be created manually in Abaqus™. Ligament placement was estimated from previous literature (Dowlatshahi;

Shmidt). The following ligaments were included in the model: the ulnar collateral proper, the radial collateral proper, the ulnar collateral accessory, the radial collateral accessory, the ulnar phalangoglenoidal, the radial phalangoglenoidal, the ulnar check rein, and the radial check rein. Each ligament was modeled using five point-to-point trusses in parallel (Gislason).

The volar plate and palmar plate of the joint capsule were modeled using ten and thirteen point-to-point trusses respectively (Gislason). In addition, another thirteen point-to-point trusses were used to represent the radial and ulnar side of the joint capsule, separate from the two plates (Gislason).

The sesamoids are embedded in the palmar plate of the joint capsule, and had to be modeled as such (Shmidt). This was simulated by creating ten point-to-point trusses on each sesamoid, five of which attach to the metacarpal head and five of which attach to the base of the proximal phalanx (Gislason).

Three tendons were included in this model: the flexor pollicus brevis, the abductor pollicis brevis, and the adductor pollicis. These tendons play a crucial role in the stability of the proximal phalanx and the sesamoid bones (Shmidt). The FPB and APB both insert into the left lateral portion of the base of the proximal phalanx, and the ADP inserts into the right. For simplicity, the FPB and APB were combined and represented as one point-to-point truss, with one point fixed to a node below the metacarpal head. The ADP was also represented as such.

Cartilage is present at the contact points of the metacarpal and the proximal phalanx. To accurately model it, the surfaces of the bones were both extruded 0.3mm (Gislason).

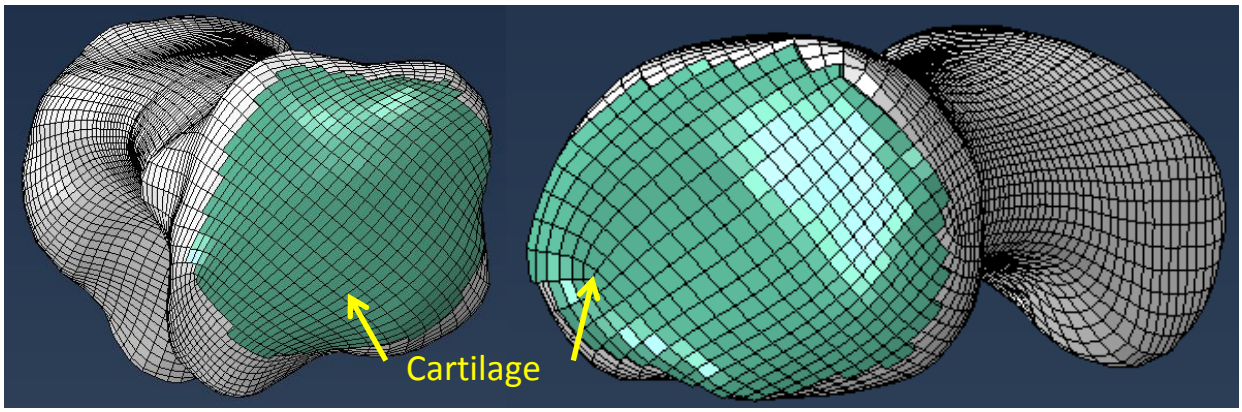

Figure 4-9: Location and Distribution of Cartilage on the Proximal Phalanx and Metacarpal

4.5.4 Assigning Material Properties

4.5.4.1 Cancellous and Cortical Bone

Since bone is composed of both cortical and cancellous portions that have separate mechanical properties, using a uniform distribution of material across each bone would not provide an accurate model. The distribution of cortical and cancellous bone was determined from the CT scan images; the lighter portion indicates cortical bone and the darker portions indicate cancellous bone.

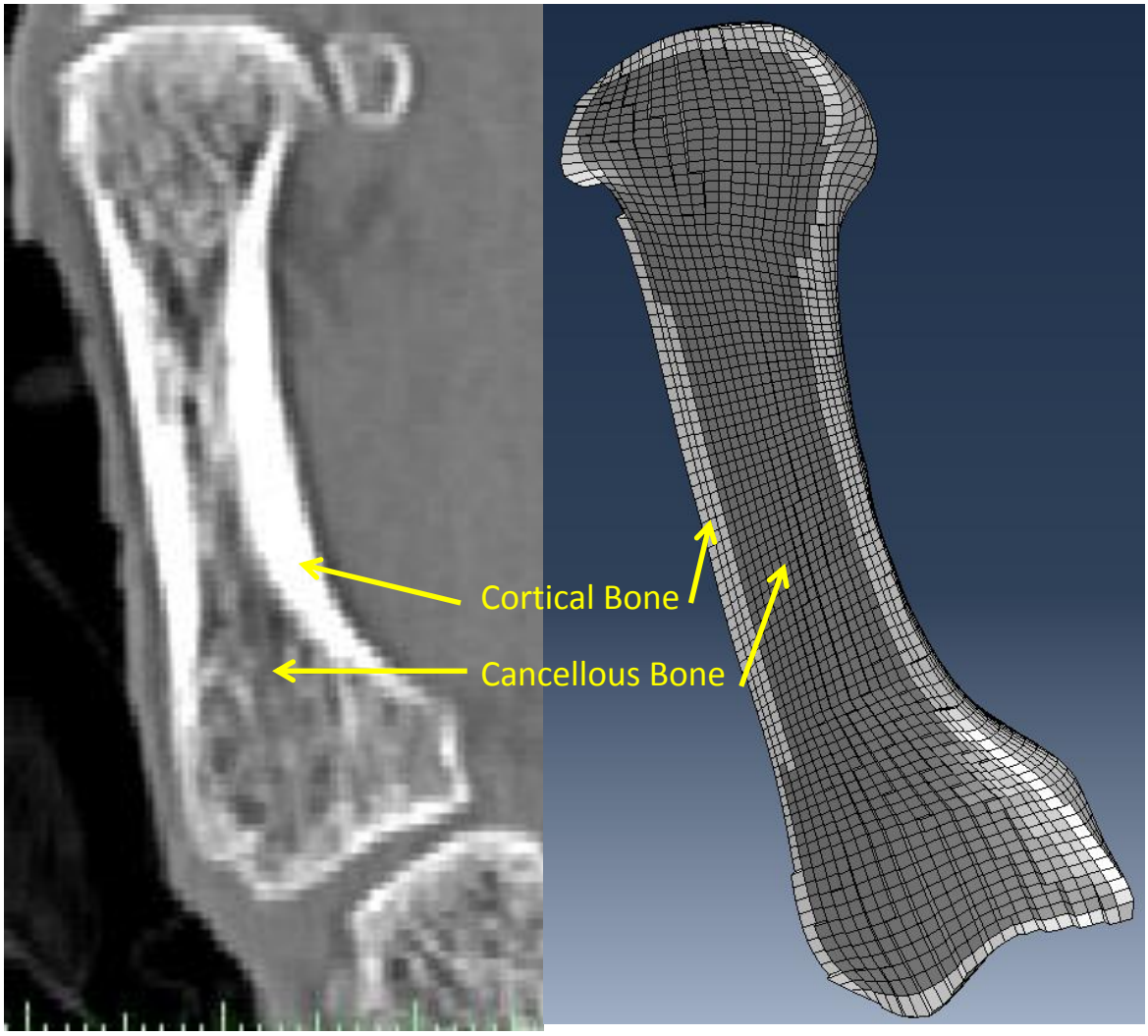

Figure 4-10: Distribution of the Cortical and Cancellous Bone

Characterizing the exact material properties of bone is difficult due to the variability between publications. This can be attributed to several factors such as bone size, function, position, age of the subject, and variability of testing methods. Even two separate experiments performed by the same group yielded significant differences. In one study using nanoindentation to measure Young's Modulus, the average was 13.4 +/- 2.0 GPa for cancellous bone and 25.8 +/- 0.7 GPa in cortical bone (Rho "Elastic Properties of Human Cortical and Trabecular Lamellar Bone Measured by Nanoindentation"). The

second study utilized ultrasonic and microtensile testing. Young's modulus for cancellous bone was 14.8 +/- 1.4 GPa and 10.4 +/- 3.5 GPa; for cortical bone it was 20.7 +/- 1.9 GPa and 18.6+/- 3.5 GPa for ultrasonic and microtensile testing respectively (Rho "Young's Modulus of Trabecular and Cortical Bone Material: Ultrasonic and Microtensile Measurements"). Values for Poisson's ratio range from 0.2 to 0.3 depending on the study (Yoganandan), (Gislason), (Ha), (Hu).

Three publications regarding FEA analysis have used 100 MPa for the Young's Modulus of cancellous bone, a value that is indicative of an average of different studies and the one that was selected for our model (Yoganandan), (Gislason), (Ha). Cortical bone has been reported with a Young's modulus of 10 GPa, 18 GPa, and 19.7 GPa by (Yoganandan), (Gislason), and (Currey) respectively. An average of 16 GPa was used in our model. Although there was some variability in the reported Poisson's Ratio, multiple studies reported that both cancellous and cortical bone have a value of 0.29 (Yoganandan), (Hu), (Ha). This value was used for both types of bone in the model. Most FEA studies model both types of bone as isotropic and linear elastic. These properties will also be applied to both cortical and cancellous bone.

4.5.4.2 Ligaments

There is limited documentation of the mechanical properties of the metacarpal phalangeal joint. The only ligament that has been reported on is the ulnar collateral ligament, and it was conducted *in vi*tro (Firoozbakhsh). Although the properties found from the study could be attributed to all of the capsular ligaments, this would require a linear elastic model to be used. Ligamentous material is most often characterized with either viscoelastic or hyperelastic models, as its complex structure makes a linear elastic model insufficient. The ligaments will be characterized using a strain energy density function of an incompressible Neo-Hookean material shown in Equation 4-1: Neo-Hookean Strain Energy

Density Function, where C_1 is the initial shear modulus and I_1 is the first modified invariant of the right Cauchy-Green strain tensor (Pena).

Equation 4-1: Neo-Hookean Strain Energy Density Function

$$\Psi = C_1(I_1 - 3)$$

C_1=6 MPa for ligaments of this model, which has been shown through other studies to represent ligamentous material (Pena), (Perez del Palomar).

4.5.4.3 Cartilage

The cartilage was modeled using the Mooney-Rivlin strain energy density function for an incompressible hyperelastic model. Linear elastic models can only accurately predict smaller deformation behavior, up to an elastic strain rate of approximately 5% (Gislason). A hyperelastic deformation model will be better suited to the model, because the cartilage will be undergoing very high strain rates during impact loading. The strain energy density function for a two parameter Moon-Rivlin model is shown in Equation 4-2.

Equation 4-2: Incompressible Strain Energy Density Function

$$W = C_1(I_1 - 3) + C_1(I_2 - 3)$$

The values for the coefficients are taken from previous work modeling articular cartilage, with C_{01}=0.41 MPa and C_{10}=4.1 MPa (Li).

4.5.4.4 Tendons

The range of reported Young's Modulus for tendons is very large, particularly when comparing *in vitro* and *in vivo* measurements. Reported values for *in vitro* measurements are in the range 350 MPa to 850 MPa; *in vivo* values are far greater, ranging from 1,000 MPa to 2,000 MPa. This large increase is

most likely due to the support of the surrounding tissue of the tendon *in vivo*. Values reported for the flexor pollicis longus *in vitro* range up to 1,000 MPa when the tendon is subjected to 15 MPa of stress. The project team assumed that the smaller size of the tendons in the model, the Young's Modulus would be lower, and a value of 280 MPa was chosen. A value of 0.49 was chosen for Poisson's Ratio based off of previous finite element analysis work done on the shoulder.

4.5.4.5 Volar and Palmar Plates

The volar and palmar plates of the MPJ are fibrocartilagenous material, and therefore cannot be represented in the same manner as articular cartilage. The region of the material affects its mechanical properties, and makes it difficult to attribute specific values. An average of the mechanical properties was used, with a Young's Modulus of 6 MPa and a Poisson's Ratio of 0.4.

4.5.5 Creating the Steps

Abaqus™ runs simulations by utilizing a series of different steps. For the model, two steps were created: one for preloading and one for applying the force from the ball. During the preloading step, the proximal phalanx was subjected to one Newton of force at the distal articular surface of its head. This step ensures that the proximal phalanx and metacarpal are in contact before the real load is applied. The second step mimics the force exerted onto the thumb when a goalkeeper catches a ball. The force is applied at the right lateral portion of the distal end of the proximal phalanx. The force was varied in order to achieve a wide range of results.

4.5.6 Constraints and Boundary Conditions

In order to ensure that the model will behave like the metacarpal phalangeal joint when subjected to a specific load, boundary conditions and constraints had to be applied. The metacarpal was fixed at its base in both steps to prevent random movement of the system when the force was applied.

In addition, the ends of the two tendons were fixed below the palmar portion of the metacarpal head to ensure that their function as stiff supports of the proximal phalanx was achieved. During the preload step, the head of the proximal phalanx was constrained in the X and Y direction, because only movement in the Z direction was needed to initiate contact. In addition, no rotational movement was allowed, as it was also unnecessary for a contact phase. During the actual loading step, the right lateral portion of the distal end of the proximal phalanx was constrained in the Y direction. Since we are interested in the mechanism of over-abduction, constraining the Y direction will not affect the results we desire. In addition, the same area was not allowed to rotate around the X and Z axis. This was also to prevent extraneous movements of the proximal phalanx.

4.5.7 Modeling the Load

The load that was applied to the model was designed to represent the impact of a soccer ball on the goalkeepers thumb. The location of the load was estimated from Figure 2-1 as well as information obtained from our own tests catching a ball. To properly create the area of contact, a node point was created and coupled with the surfaces within the determined location. This allowed for the distribution of the load over the entire surface instead of a single point. The force that was applied to the site was determined using the impulse equation, shown in Equation 4-3. F is the force exerted by the ball on the hand, p_f is the final momentum of the ball, p_i is the initial momentum of the ball, t is the stopping time of the ball, m is the mass of the ball, v_f is the final velocity of the ball, and v_i is the initial velocity of the ball.

Equation 4-3: The Impulse Equation

$$F = \frac{p_f - p_i}{t} = \frac{mv_f - mv_i}{t}$$

A soccer ball has a dry mass of 0.45 kg. The average velocity of the ball when kicked by a professional soccer player is 31 m/s. We want this device to be able to function with a safety factor, however, so the highest recorded velocity of a kicked soccer ball was used, 39 m/s. The time of contact was assumed as 0.025 seconds, based on previous work done analyzing contact time during catching. This resulted in a net force of 702 N. Unfortunately, this high force load could not be used due to the dynamic loading restrictions of Abaqus/Standard™, and lower values were used instead (Simulia).

4.6 Preliminary Data

The model was subjected to loads of 10N, 100N, and 150N. These loads were chosen based off of *in vitro* mechanical loading of the UCL, where it was found that at 150N the UCL would experience 6.31 MPa of stress. The results for stress vs. time and strain vs. time can be seen in Figure 4-13. In addition, the stress experienced by the UCL proper, the UCL accessory, the UPL, and the CRL were all compared graphically at both 10 and 150 Newtons. Clinical data shows that the UCL is the most likely to be damaged during excessive abduction, meaning that the UCL experiences the most stress and strain (Dowlatshahi). The computed data supports this theory; at 10N, all of the ulnar ligaments experience comparable amounts of stress. At 150N, however, the UCL proper experiences stress at much higher levels than the other three ligaments.

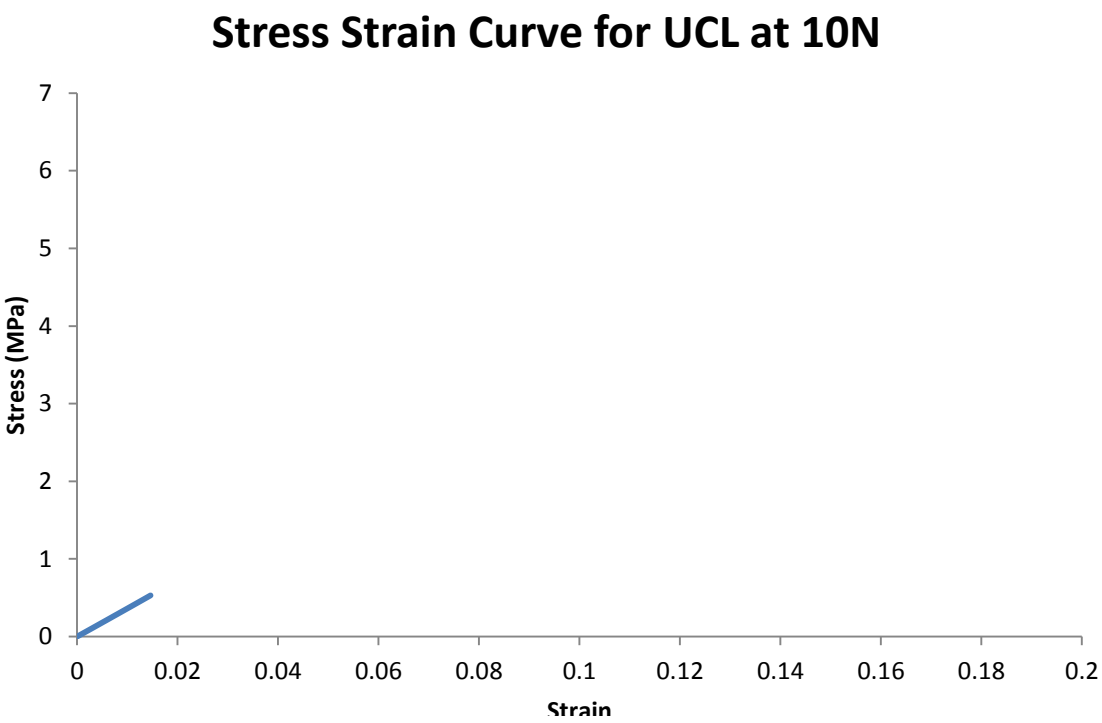

Figure 4-11: Stress Strain for the UCL at 10N

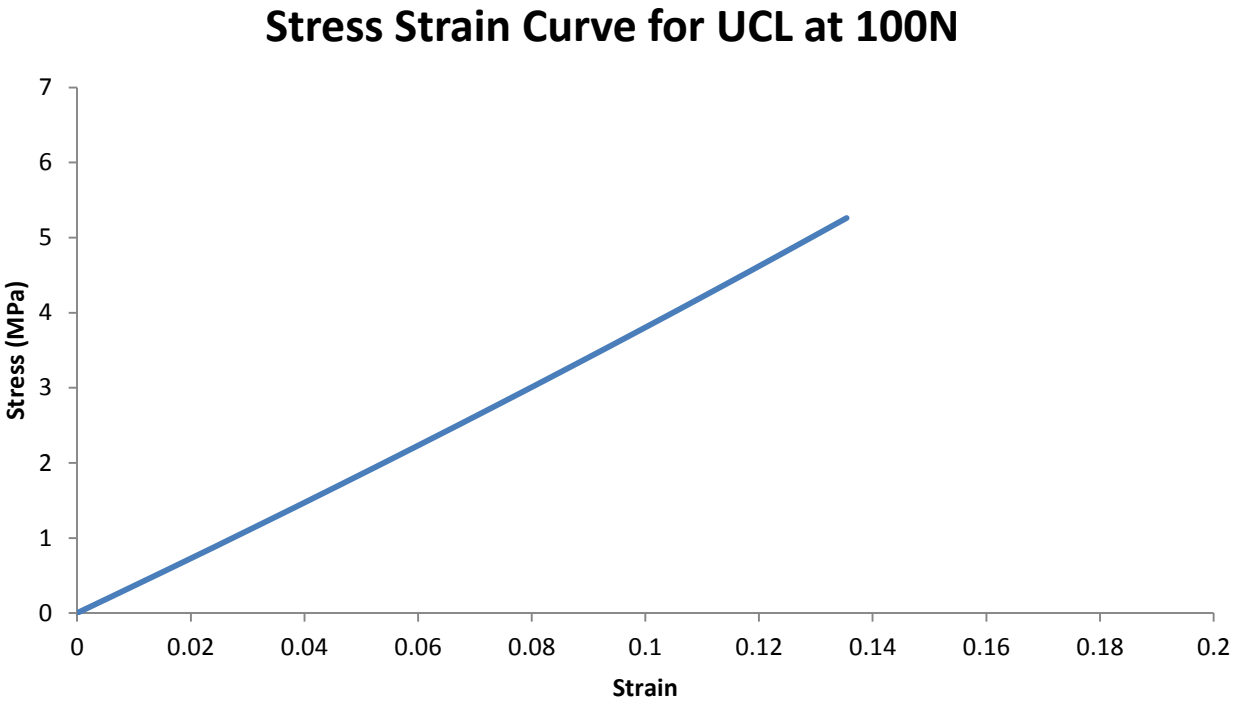

Figure 4-12: Stress Strain for the UCL at 100N

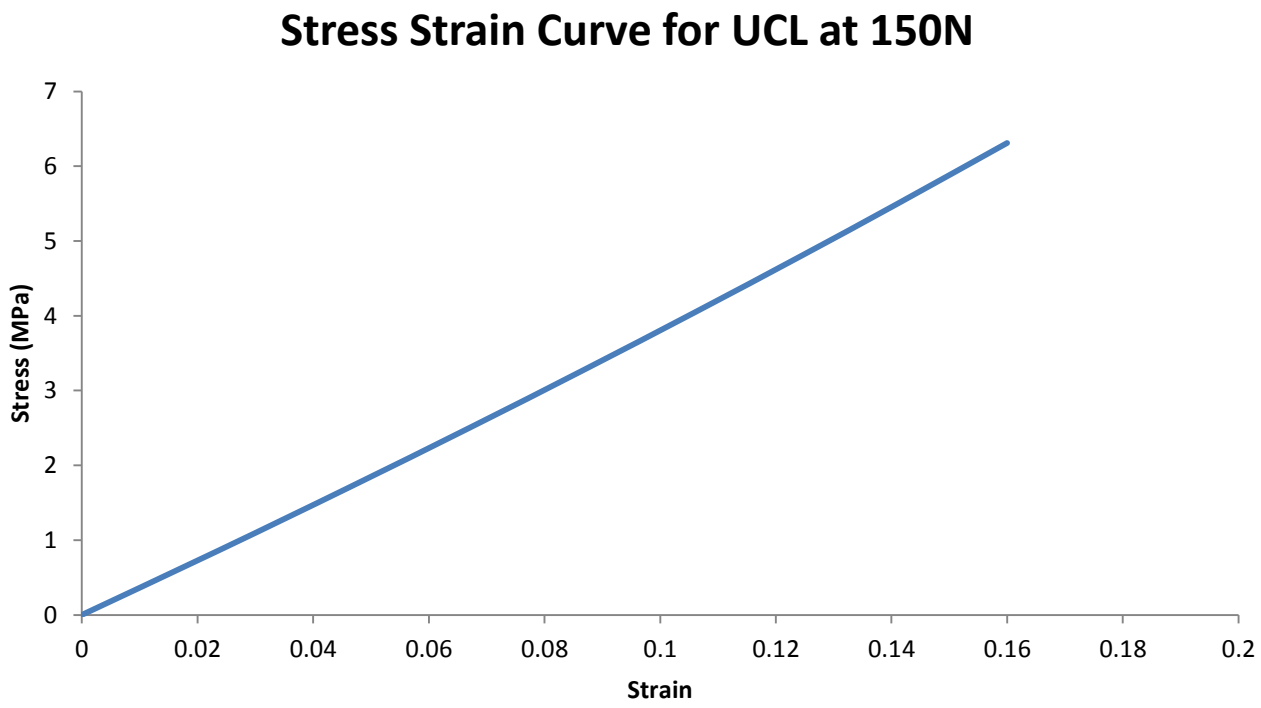

Figure 4-13: Stress Strain for the UCL at 150N

The stress-strain data for the model is the result of several assumptions made, both implicitly by Abaqus™ and explicitly. Abaqus™ assumes that the load is delivered in a ramp fashion, i.e. over the period of the step time. Abaqus/Standard™ is unable to model instantaneous loading conditions. A characteristic graph of a stress-strain curve for ligaments includes three regions: the toe region, the linear region, and the yield and failure region. The toe region represents the period during loading that the collagen fibrils of the ligament are un-crimped. The crimped fibrils have low stiffness that increases as they stretch, eventually resulting in the collagen fibril backbone being stretched. This concludes the toe region and initiates the linear region. After the linear region, the ligament reaches its yield stress and begins to plastically deform, eventually reaching its failure point. The best way to model this in Abaqus™ would be to input graphical data from mechanical testing. Unfortunately, the project team did not have access to data relevant to the UCL, so the stress-strain graph obtained by Abaqus™ represents only the linear portion.

When compared to previously published data on the mechanical properties of the UCL, the data shows that the model is an effective representation of the actual ligament. *In vitro* mechanical testing of the UCL resulted in a failure load of 294.3 +/- 28.2 N and a maximum stress of 11.4 +/- 1.2 MPa. [Figure] shows that at a load of 150N, the UCL experiences 6.3 MPa of stress, approximately half of the experimental value. Based on this data, this model will provide an effective method to test the device. The graph of the stress strain curve obtained through *in vitro* mechanical loading is shown with the computed FEA data in figure. The Young's Modulus obtained from the *in vitro* study was not used in the mechanical properties assigned in our FEA model. The graph clearly shows that the stress strain graph from the physiological FEA model is an excellent representation of the experimental data, aside from the lack of a toe region.

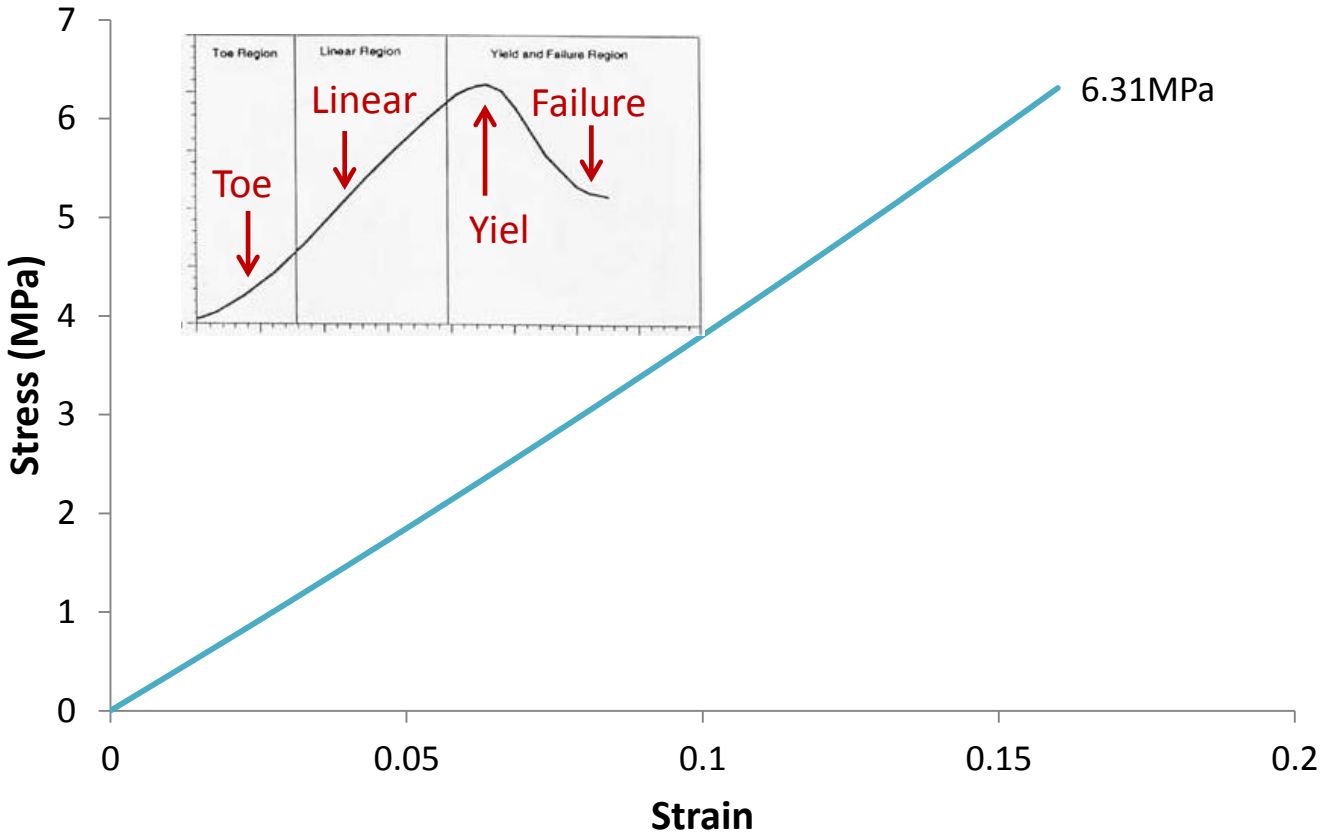

Figure 4-14: Stress Strain Curve of the UCL at 150N with Characteristic Ligament Stress Strain Behavior

5 Design Verification

The verification of the design was dependent on the validation of the physiological model, detailed in Preliminary Data. This section will explore the results obtained from the addition of the spine device into the physiological model of the MPJ.

Initially, the FEA model of the spine device was imported in full to the MPJ model. During the simulations, however, the device experienced excessive distortion and the sequence could not converge. In order to examine the reason behind the failure, the device was shortened to two parts. The piece closest to the posterior end of the metacarpal was fixed and the second piece was constrained in such a way as to only allow for rotation around the pins. By modifying the constraints and boundary conditions, one piece was successfully able to rotate around the other.

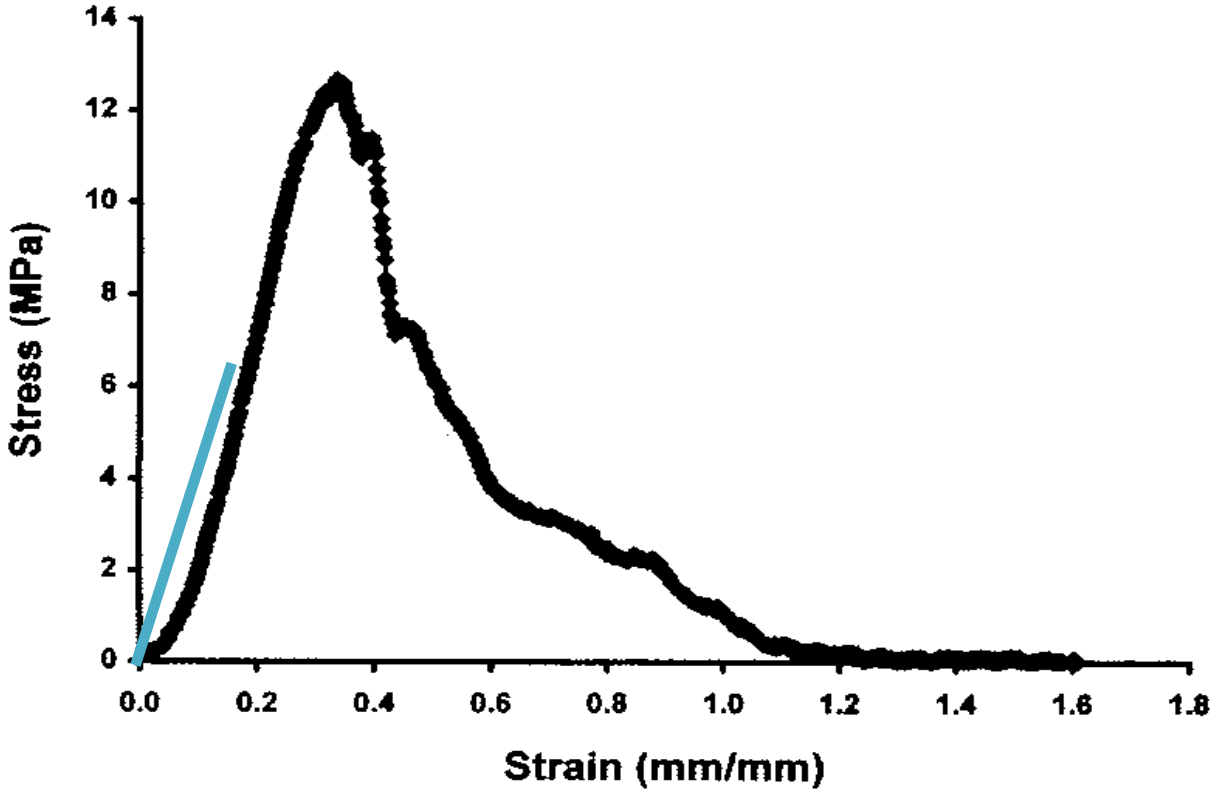

Figure 5-1: Computed Stress Strain of the UCL Compared to Experimental Data

The same conditions applied to the two piece model were then applied to a full model of the device without the MPJ. Unfortunately, these same conditions did not allow the simulation to complete. After conversing with Dr. Kiapour, the constraints and conditions were modified again and the spine was able to function effectively.

As a final step, the spine was imported into the MPJ model and positioned in a way that best resembled the actual placement of the device. The proximal phalanx was then subjected to the same 150N load as it was in the validation of just the MPJ model. The simulation was only run at 150N due to time constraints, as each simulation took approximately nine hours and there were multiple unsuccessful attempts.

Figure 5-2 shows the comparison of stress vs. time on the UCL at 150N with and without the device. Figure 5-3 and Figure 5-4 show the comparison of the stress strain curves for the UCL at 150N with and without the device. Table 5-1and Table 5-2 show the numerical data.

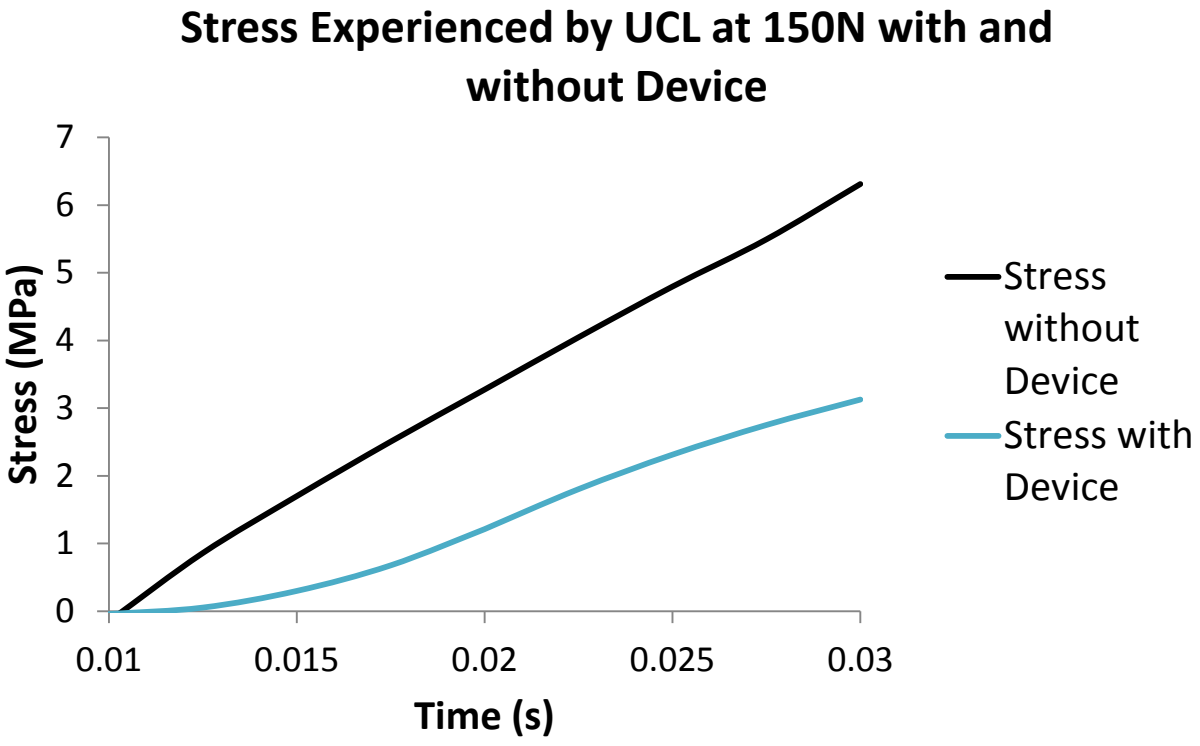

Figure 5-2: Stress Experienced by the UCL at 150N with and without the Device

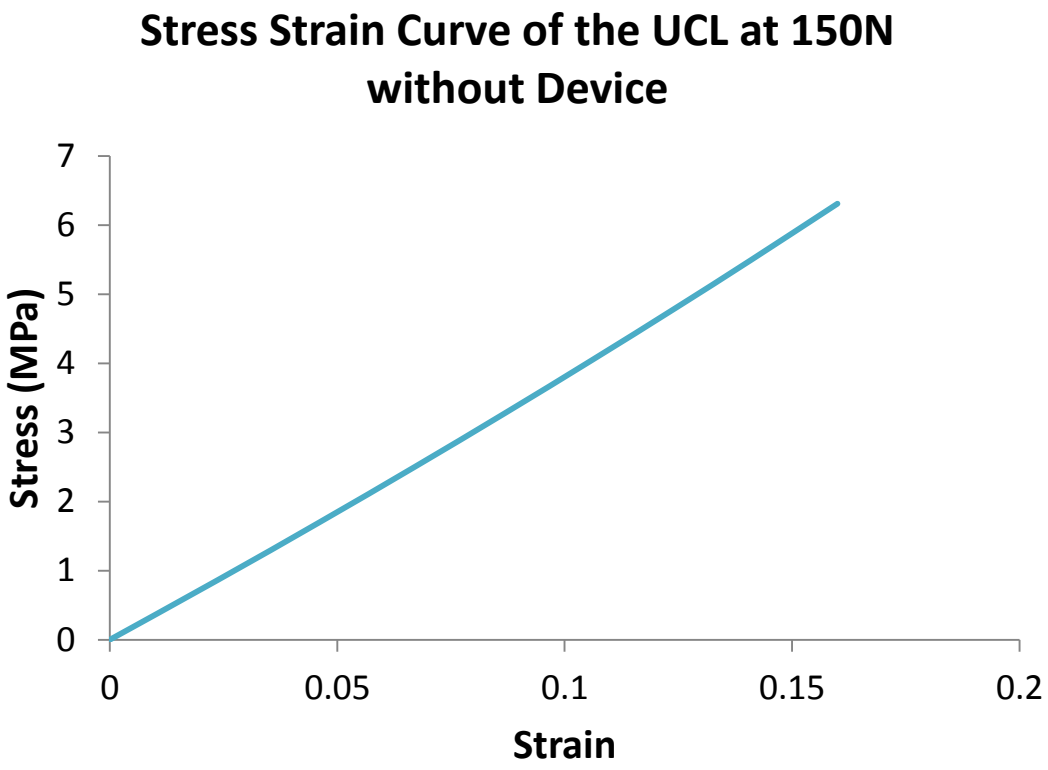

Figure 5-3: Stress Strain Curve for the UCL at 150N without the Device

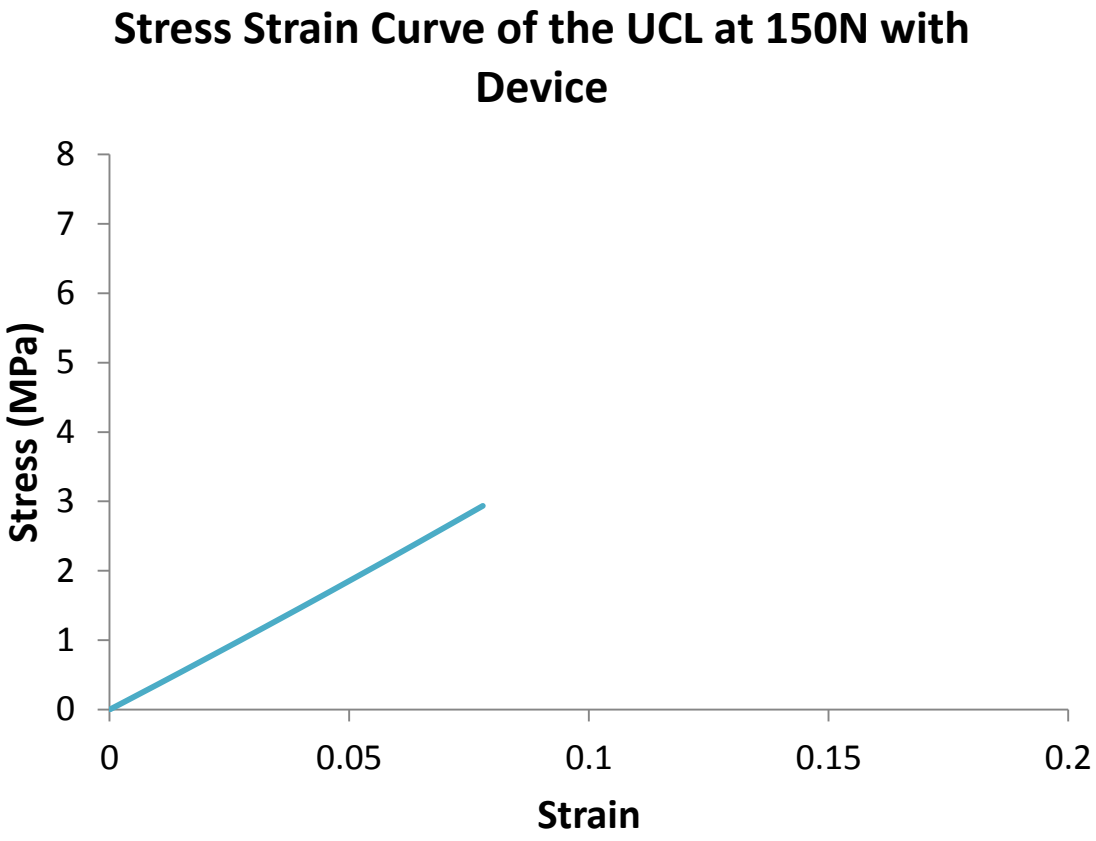

Figure 5-4: Stress Strain Curve for the UCL at 150N with the Device

UCL without Device	
Time (s)	Stress (MPa)
0.01	0.86
0.02	1.70
0.02	2.51
0.02	3.28
0.02	4.05
0.03	4.80
0.03	5.49
0.03	6.31

UCL with device	
Time (s)	Stress (MPa)
0.01	0.06
0.02	0.30
0.02	0.68
0.02	1.21
0.02	1.80
0.03	2.31
0.03	2.75
0.03	3.13

Table 5-1: Time and Stress Data for the UCL at 150N with and without the Device

UCL with Device	
Strain	Stress (Mpa)
0.02	0.86
0.05	1.70
0.07	2.51
0.09	3.28
0.11	4.05
0.12	4.80
0.14	5.49
0.16	6.31

UCL without Device	
Strain	Stress (Mpa)
0.00	0.05
0.01	0.23
0.01	0.54
0.03	1.00
0.04	1.47
0.05	1.94
0.06	2.43
0.08	2.94

Table 5-2: Stress Stress Data for the UCL at 150N with and without the Device

6 Discussion

The creation of the physiological model of the MPJ and the model of the device were both integral to the success of this project. Both models were created under a number of different assumptions. Table 6-1 shows the assumptions made during the creation of the physical model. Table 6-2 shows the assumptions made during the creation of the device model.

Assumptions	**Justifications**
Ligament, tendon, plate, and jount capsule placement was derived from literature, not MRI scans.	The MRI images were not of high enough quality to determine placement.
Ligaments were modeled as bundles of 5 wires with consistent cross sectional areas.	This modeling method is based off of previous work done on the wrist (Gislason).
The volar plate was modeled as a bundle of 10 wires with consistent cross sectional areas.	This modeling method was based off of previous work done on the wrist (Gislason).
The palmar plate was modeld as a bundle of 13 wires with consistent cross sectional areas.	This modeling method was based off of previous work done on the wrist (Gislason).
The joint capsule was modeled as a bundle of 13 wires with consistent cross sectional areas.	This modeling method was based off of previous work done on the wrist (Gislason).
The tendons were modeled as point to ground wires.	The origin sites of the tendons are not present in the model so they are modeled in the directions that they provide stability (Shmidt).
Ignored skin, subcutaneous fat, etc.	These structures provide minimal support and could not be modeled in the time allotted (Shmidt; Dowlatshahi; Petre; Smutz).
The base of the metacarpal was fixed.	The base of the metacarpal must be fixed to prevent the model system from floating (Simulia).

The area of the impact force was applied at a node coupled to multiple surface elements.	The impact region was derived from X-ray images of a hand holding a ball as well as our own physical tests (Dowlatshahi).
The movement of the proximal phalanx was constrained in the Y direction.	This will allow for simulation of the abduction motion of interest.
The rotation of the proximal phalanx was constrained around the X and Z axis.	This will allow for simulation of the abduction motion of interest.
Assumed bone is isotropic	This assumption has been made in several other finite element analysis studies (Firoozbakhsh; Gislason; Ha; Hu; Li).
Assumed constant strain rate	A variable strain rate was outside of the computational ability of Abaqus/Standard (Simulia).
The effects of temperature were ignored	Although temperature does have a small effect on the properties of tissue, it is negligible in our model

Table 6-1: Assumptions Made for the Physiological Model

Assumptions	**Justifications**
The piece of the device at the base of the metacarpal was fixed.	Part of the device had to be fixed in space to prevent it from floating.
The model was not placed entirely flush against the MPJ.	The exclusion of skin in the model made it impossible to have the device in its exactly correct position.
Direct, non-penalty contact was used for the device pieces.	This contact method best simulates the actual interactions between the device pieces.
Poor quality mesh was assigned to the device pieces.	Abaqus Student Edition only allows for 100,000 nodes in the model.

Table 6-2: Assumptions Made for the Device

Most test methods for determining mechanical properties of soft tissue are done on cadaveric tissue that has been frozen for a period of time; in addition, available cadaveric tissue typically comes from older subjects. This leads to inaccurate results for these properties, because the properties of soft

tissues degrade noticeably with age. These properties and their rationales were discussed previously in Chapter Four. The assumptions of mechanical properties for the different tissues allowed for the successful validation of the physiological model.

The device was modeled using the mechanical properties for Pebax®, which would be the material of choice for production. After being inserted into the model adjacent to the MPJ, the MPJ was subjected to a load of 150N. This load caused it to deviate radially and contact the spine. The spine was positioned as accurately as possible, taking into account its placement as a possible source of error. The skin of the MPJ was not included in the model, and the device would ideally be placed directly in contact over the entire surface. The shape of the bones made it impossible to position the device in direct contact at all points, so the spine was not able to lock up as early on as it would during normal use.

The comparison of the stress vs. time graphs for 150N with and without the device can be seen in Figure 5-2 of the results section. Early on, the curve with the device begins to deviate from the curve without the device. This is due to the initial contact of the proximal phalanx with the spine. This trend of less stress and strain continues, and as the spine locks up fully, the curve begins to level off. The comparison of the stress strain graphs for 150N with and without the device can be seen in Figure 5-3 and Figure 5-4 of the results section. The stress strain curve with the device shows a clear decrease in both how much stress and strain is experienced by the UCL, which would result in a lower chance of injury for the UCL.

Previous work done in this area has shown that the addition of a goalkeeping glove lessens the chance of injury to the UCL, but not by a significant amount (Dowlatshahi). The work presented here shows that with the device in place, the UCL experiences approximately half as much stress and strain, drastically reducing the likelihood of injury.

6.1 Environmental Impact

By using Pebex® Rnew, the impact on the environment is drastically reduced. It allows for a 29% reduction in fossil energy used and 32% of CO2 emissions. Although the production of it will still create CO2 and require the burning of fossil fuels, this eco-friendly material will drastically reduce the impact on the environment (Arkema).

6.2 Societal Influence

The production of this device would create more jobs, as this device would be produced on a fairly large scale. In addition, fewer injuries would occur, effectively reducing health care needed by soccer goalkeepers. Reduced risk of injury would allow goalkeepers to play more without having to worry about a possible injury threatening their ability to play.

6.3 Ethical Concern

The design of the device does not use any ethically concerning methods or materials. The device is meant to protect the user from harm while participating in the sport of intended use.

6.4 Economic Impact

The results of this project will most likely not have a significant impact on the economy of everyday living. If the device was patented and sold to a large sports company, such as Nike® or Adidas®, it could be integrated into their high-end goalkeeping gloves and marketed to the professional soccer community. This would have a sizeable impact on the economics of professional soccer equipment, but in the grand scheme of the economy it would most likely have a minimal effect.

6.5 Political Impact

In many countries worldwide, soccer is the most played and most watched sport. Although this device is not intended for younger players, mostly due to a lack of need, it could have a large effect on the way professional goalkeepers purchase gloves. The decreased chance of injury that results from the introduction of the device into a goalkeeping glove could be very important to professional goalkeepers. Injuries to the UCL can cause a goalkeeper to be benched and lose their starting position, which would be devastating for their career. This spine device would allow goalkeepers to keep their positions by lessening their risk of injury.

6.6 Health and Safety Issue

The purpose of this spine is to increase the personal safety of soccer goalkeepers. The spine prevents over-abduction of the MPJ, which in turn reduces the chance of injury to the UCL and the other structures of the joint. In severe cases, injury to the MPJ can require long recovery times and surgical intervention. The reduced risk of injury will be beneficial to the safety of goalkeepers.

6.7 Manufacturability

The proof of concept of the device was created using rapid prototyping, but on a large production scale, injection molding would be ideal. The initial cost of the mold would be high, but it would allow the device to be produced quickly, efficiently, and cheaply. The ideal material for commercialization of the device is Pebax® because of its low cost and previous utilization in high performance sports equipment (Arkema).

7 Final Design and Validation

From the evaluations of the preliminary designs, two designs were chosen for modeling in SolidWorks™. The first design, referred to as the "vertebrae" design, consists of a number of interlocking pieces that prevent over-abduction of the MPJ. As the pieces completely enclose the thumb, it would be difficult to size this design properly for different users.

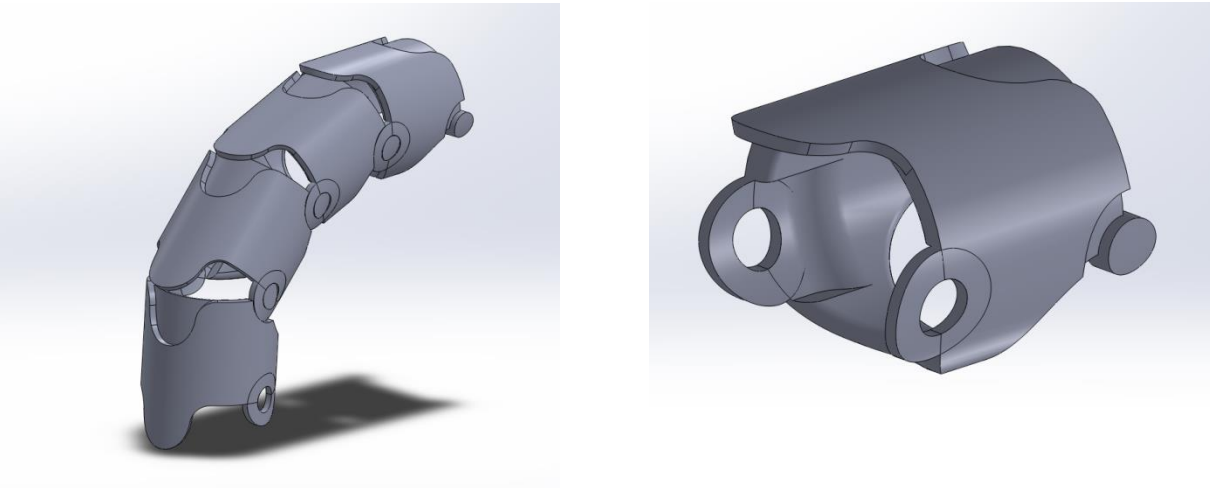

Figure 7-1: Full vertebrae and vertebrae piece

The other SolidWorks™ design, a “spine”, incorporated a series of interlocking pieces that also prevent over-abduction of the MPJ without enclosing the thumb.

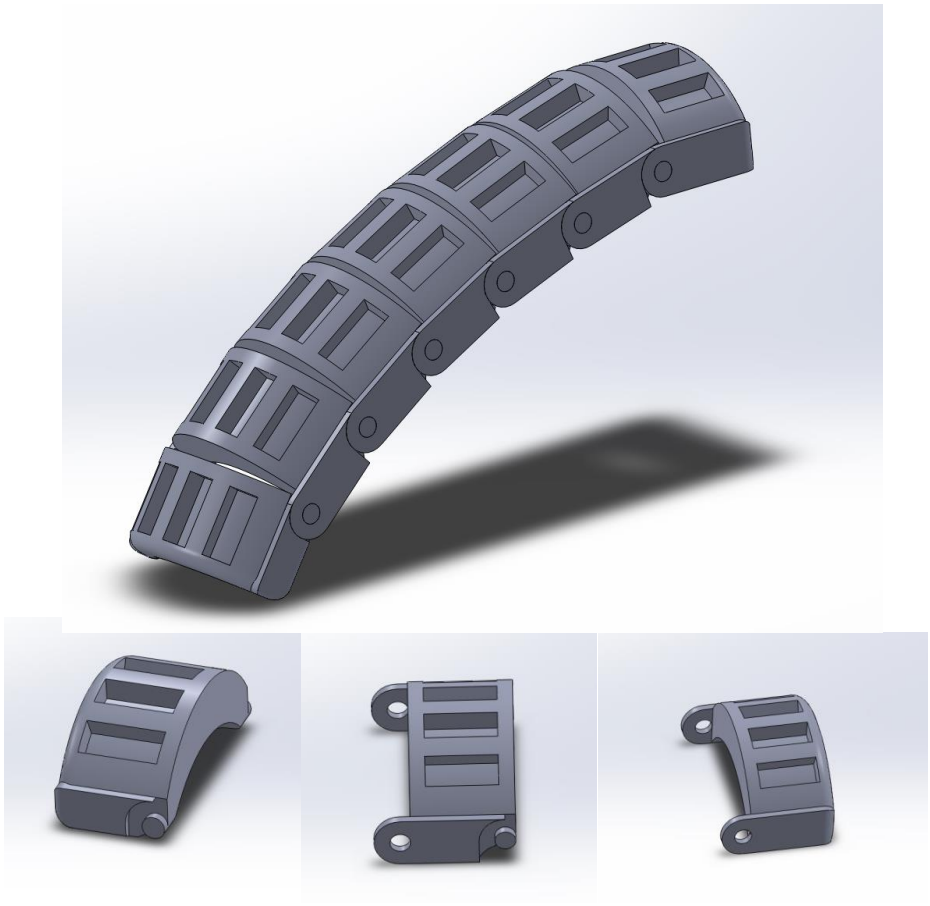

Figure 7-2: Spine Design with Pieces

The first mock-up of the “spine” design consists of seven (7) interlocking parts, with one (1) top piece, one (1) bottom piece, and five (5), middle pieces. The middle pieces consist of both an attachment pin and a receiving end to allow for rotation when connected. The pieces were submitted as .STL files to the Rapid Prototyping Lab at WPI. The parts were manufactured using ABS plastic with a Dimension SST 1200 ES Rapid Prototype Machine.

Figure 7-3: Full and Zoomed in View of the First Prototype

The first prototype was not reproduced very accurately by the Dimension SST 1200ES Rapid Prototype Machine, and inspired changes in the SolidWorks™ model for the second prototype. Soon after its manufacture, new part guidelines for recommended minimum dimensions for element thickness were posted. The pin and receiving elements of the parts were smaller than the newly recommended 0.045". By increasing the size of both the pin and receiving elements of the part, the second prototype was accurately reproduced. The device was printed entirely as an assembly using the Object260 Connex Rapid Prototype Machine with VeroWhite Polyjet Resin. Clearance of 0.01" was left between all contact surfaces in order to allow for free movement.

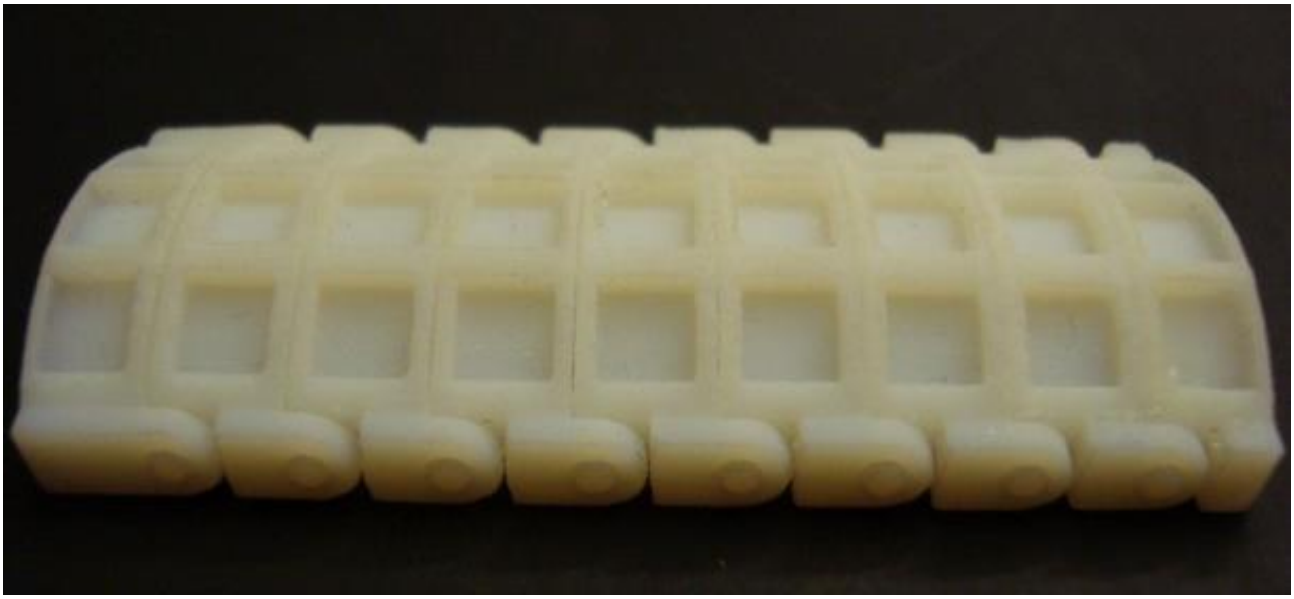

Figure 7-4: Second Prototype with Successful Attachment Points

The second prototype served as the proof of concept for the device, validating that the SolidWorks design could be manufactured properly into a working prototype. In order to allow for the insertion of the device into a goalkeeper glove, the final design was extended. It consists of fifteen (15) interlocking pieces. Thirteen (13) are identical middle pieces, with the bottom piece designed to be secured in the wrist strap of the glove, and the top piece secured at the top of the thumb. This will keep the device firmly in place against the thumb, ensuring its effectiveness.

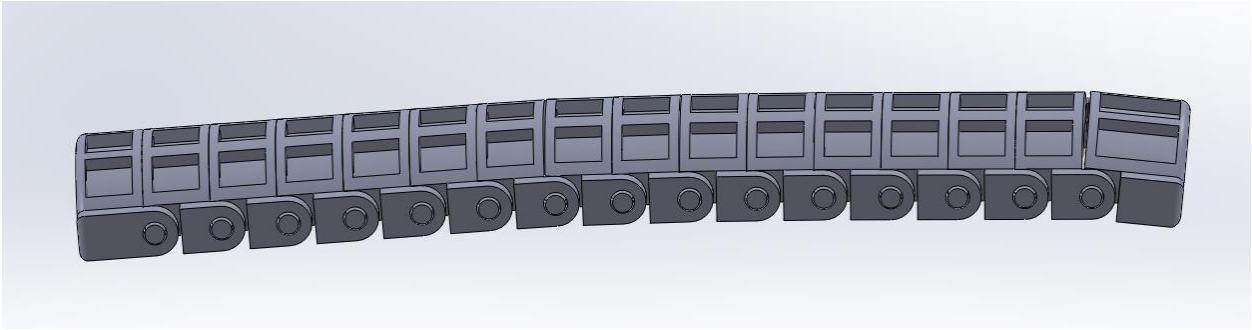

Figure 7-5: Final Spine Device

The final device consists of fifteen (15) interlocking pieces. Thirteen (13) are the identical middle pieces, with the bottom piece designed to be secured in the wrist strap of the glove, and the top piece secured at the top of the thumb.

8 Conclusion and Recommendations

In meeting the project objectives, a protective device was made to lessen the stress and strain on the UCL of the MPJ of the thumb. A model of the MPJ was constructed in Abaqus™ using image data from Computed Tomography images of the forearm obtained from the NIH. The soft tissue was modeled using information from medical texts and cadaveric study, with material properties assigned according to previous finite element analysis studies due to limited available information on the mechanical properties of the tissues in the MPJ. After subjecting the computer model to various loading conditions, the computed stress and strain were validated by the available information on experimental stress and strain data.

The SolidWorks™ model of the device was imported into Abaqus™ and applied to the MPJ, and the system of joint and device were subjected to the same loading conditions. The UCL was shown to experience a clear decrease in stress over time when the device was introduced into the model. The stress vs. strain curve in the UCL also shows a noticeable decrease with the device included. Based on these results, the spine device functions as it should and reduces the risk of injury to the UCL.

After validation of the device's functionality, a Rapid Prototyped proof of concept was manufactured using VeroWhite Polyjet Resin. The material properties used in the model of the device were for Pebax® Polyether Block Amide, the desired material for commercialization of the product.

The design process for the protective device began empirically due to time constraints. The device was calculated to theoretically reduce the forces on the UCL under high impact loading conditions, but revisions could be made to the final design using the finite element analysis model in order to maximize protection without compromising mobility of the joint.

The calculated reduction in force due to the introduction of the spine device in the MPJ could be experimentally validated by human test subjects. Strain gauges and mechanical stress sensors can measure forces experienced in practice, and this human trial data could validate the usefulness of our device.

Most importantly, the process established in the project to create a finite element analysis model from CT scans can be applied for further research on the MPJ or other joints in the body for further applications. FEA analysis of joint function is an ideal way to test any device without the need for actual human subjects. This is incredibly beneficial because it reduces subjects needed, FDA approvals, and general time constraints.

Bibliography

(!!! INVALID CITATION !!!). Print.

Arkema. "Sustainability without Compromise." (2013). Web.

Avis, Richard; Boyer, Clancy; Fisher, Sam. Soccer Glove. 2011.

Benjamin, M.; Evans, E.J. "Fibrocartilage." *Journal of Anatomy* 171 (1990): 1-15. Print.

Brown, Michael G. Thumb Protector. 1991.

Carlson, Michelle Gerwin; Warner, Kristin K.; Meyers, Kathleen N.; Hearns, Krystle A.; Kok, Peter L. "Anatomy of the Thumb." *The Journal of Hand Surgery* 37.10 (2012): 2021-26. Print.

Cluett, Jonathan. "Gamekeeper's Thumb." *Orthopedics*. 2009.

Currey, J. *Handbook of Biomaterial Properties*. Ed. Black, Jonathan; Hastings, Garth: Chapman & Hall, 1998. Print.

Dowlatshahi, A.S.; Rothkopf, D.M. "Biomechanics, Treatment, and Prevention of Acute Thumb Injuries in Soccer Goalkeeper." (2010). Print.

Firoozbakhsh, Keikhosrow; Yi, In Sok; Moneim, Moheb S.; Umada, Yuji. "A Study of Ulnar Collateral Ligament of the Thumb Metacarpophalangeal Joint." *Clinical Orthopaedics & Related Research* 403.1 (2002): 247-53. Print.

Fisher, Sam; Spampinato, Antonio, Avis, Richard. Glove with Support System. Patent 7958568. 2011.

Gislason, Magnus K.; Stansfield, Benedict; Nash, David H. "Finite Element Model Creation and Stability Considerations of Complex Biological Articulation: The Human Wrist Joint." *Medical Engineering & Physics* 32.5 (2010): 523-31. Print.

Grahame, Anthony. "The History of Soccer Goalie Gloves." Livestrong.com 2011.

Ha, Sung Kyu. "Finite Element Modeling of Multi-Level Cervical Spinal Segments (C3–C6) and Biomechanical Analysis of an Elastomer-Type Prosthetic Disc." *Medical Engineering & Physics* 28.6 (2006): 531-38. Print.

Hochmuth, Peter. Goalkeeper's Glove with a Gusset. 2003.

Hu, Kai; Qiguo, Rong; Fang, Jing; Mao, Jeremy J. "Effects of Condylar Fibrocartilage on the Biomechanical Loading of the Human Temporomandibular Joint in a Three-Dimensional, Nonlinear Finite Element Model." *Medical Engineering & Physics* 25.2 (2003): 107-13. Print.

Li, Zuoping; Kim, Jong-Eun; Davidson, James S.; Etheridge, Brandon S.; Alonso, Jorge E.; Eberhardt, Alan W. "Biomechanical Response of the Pubic Symphysis in Lateral Pelvic Impacts: A Finite Element Study." *Journal of Biomechanics* 40.12 (2007): 2758-66. Print.

Malik, A.K.; Morris, T.; Chou, D; Sorene, E.; Taylor, E. "Clinical Testing of Ulnar Collateral Ligament Injuries of the Thumb." *The Journal of Hand Surgery Europe* 34.3 (2009): 363-66. Print.

Patel, Shelain; Potty, Anish; Taylor, Emma J.; Sorene, Elliot D. "Collateral Ligament Injuries of the Metacarpophalangeal Joint of the Thumb: A Treatment Algorithm." *Strategies in Trauma and Limb Reconstruction* 5.1 (2010): 1-10. Print.

Pena, E.; Calvo, B.; Martinez, M.A.; Palanca, D.; Doblare, M. "Finite Element Analysis of the Effect of Meniscal Tears and Meniscectomies on Human Knee Biomechanics." *Clinical Biomechanics* 20.5 (2005): 498-507. Print.

Perez del Palomar, A.; Doblare, M. "Finite Element Analysis of the Temporomandibular Joint During Lateral Excursions of the Mandible." *Journal of Biomechanics* 39.12 (2006): 2153-63. Print.

Petre, Benjamin McVay. "Metacarpophalangeal and Interphalangeal Ligament Anatomy." *Drugs, Diseases, & Procedures*. Medscape 2011.

Primiano, George A.; Primiano, Frank P. Jr. Safety Glove with Modified Dorsal Thumb Spica Brace. 1985.

Rho, J.Y.; Ashman, R.B.; Turner, C.H. "Elastic Properties of Human Cortical and Trabecular Lamellar Bone Measured by Nanoindentation." *Biomaterials* 18.20 (1997): 1325-30. Print.

---. "Young's Modulus of Trabecular and Cortical Bone Material: Ultrasonic and Microtensile Measurements." *Journal of Biomechanics* 26.2 (1993): 111-18. Print.

Roughley, P.J. "The Structure and Function of Cartilage Proteoglycans." *European Cells and Materials* 12 (2006): 92-101. Print.

Shmidt, Hans-Martin; Lanz, Ulrich. "Surgical Anatomy of the Hand." 2003. 84-113. Print.

Simulia. *Abaqus 6.12 User's Manual*. Print.

Smutz, Paul W.; Kongsayreeponga, Apichai; Hughesa, Richard E.; Niebura, Glen; Cooneya, William P.; Ana, Kai-Nan. "Mechanical Advantage of the Thumb Muscles." *Journal of Biomechanics* 31.6 (1998): 565-70. Print.

Yoganandan, N.; Kumaresan, S.C.; Voo, Liming; Pintar, F.A.; Larson, S.J. "Finite Element Modeling of the C4-C6 Cervical Spine Unit." *Medical Engineering & Physics* 18.7 (1995): 569-74. Print.

Yoshida, Ryol; House, Hugh; Patterson, Rita; Sha, Munir; Viegas, Steven. "Motion and Morphology of the Thumb Metacarpophalangeal Joint." *The Journal of Hand Surgery* 28.5 (2003): 752-57. Print.

Appendix A: Surface, Block, and Mesh of the Metacarpal

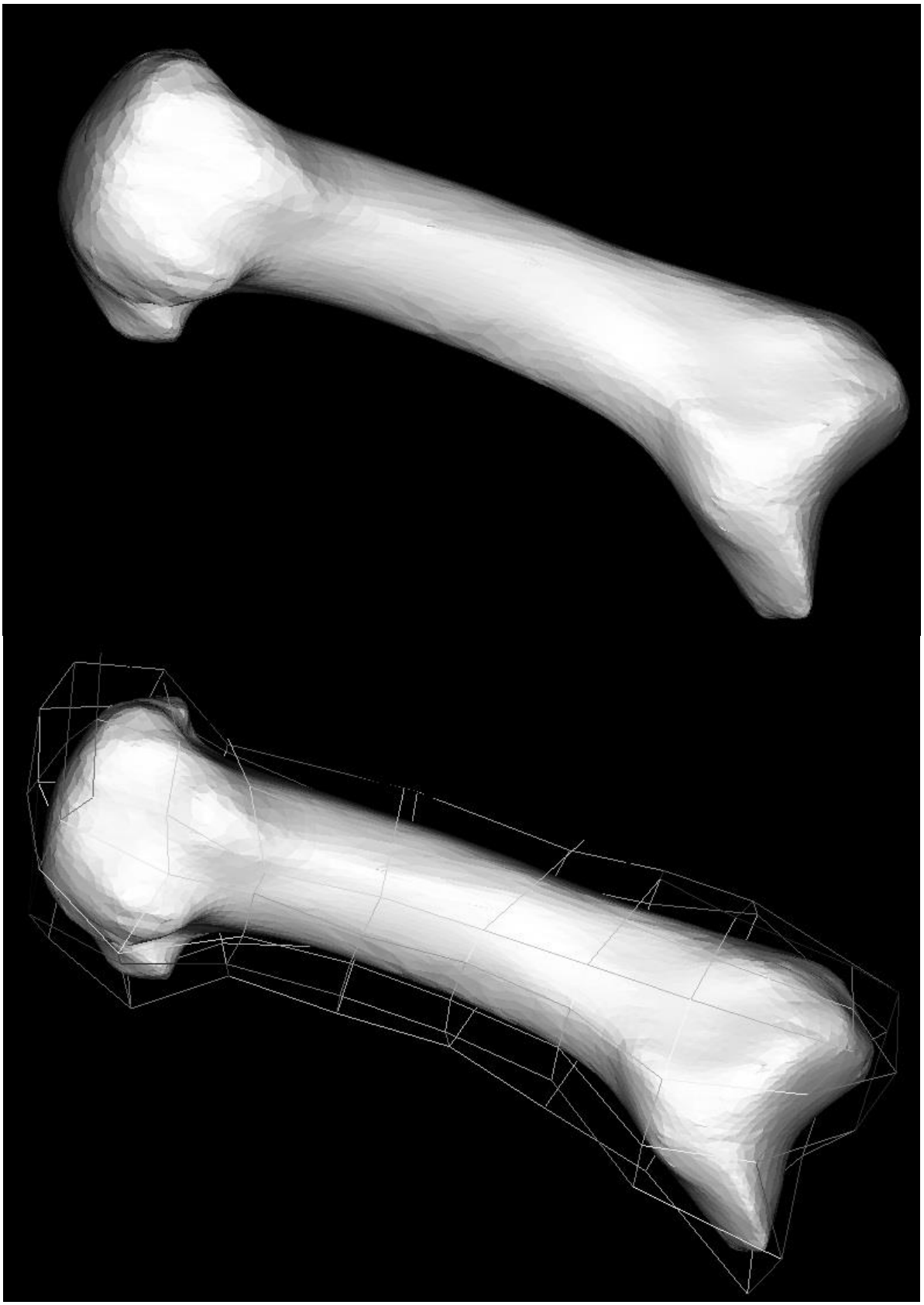

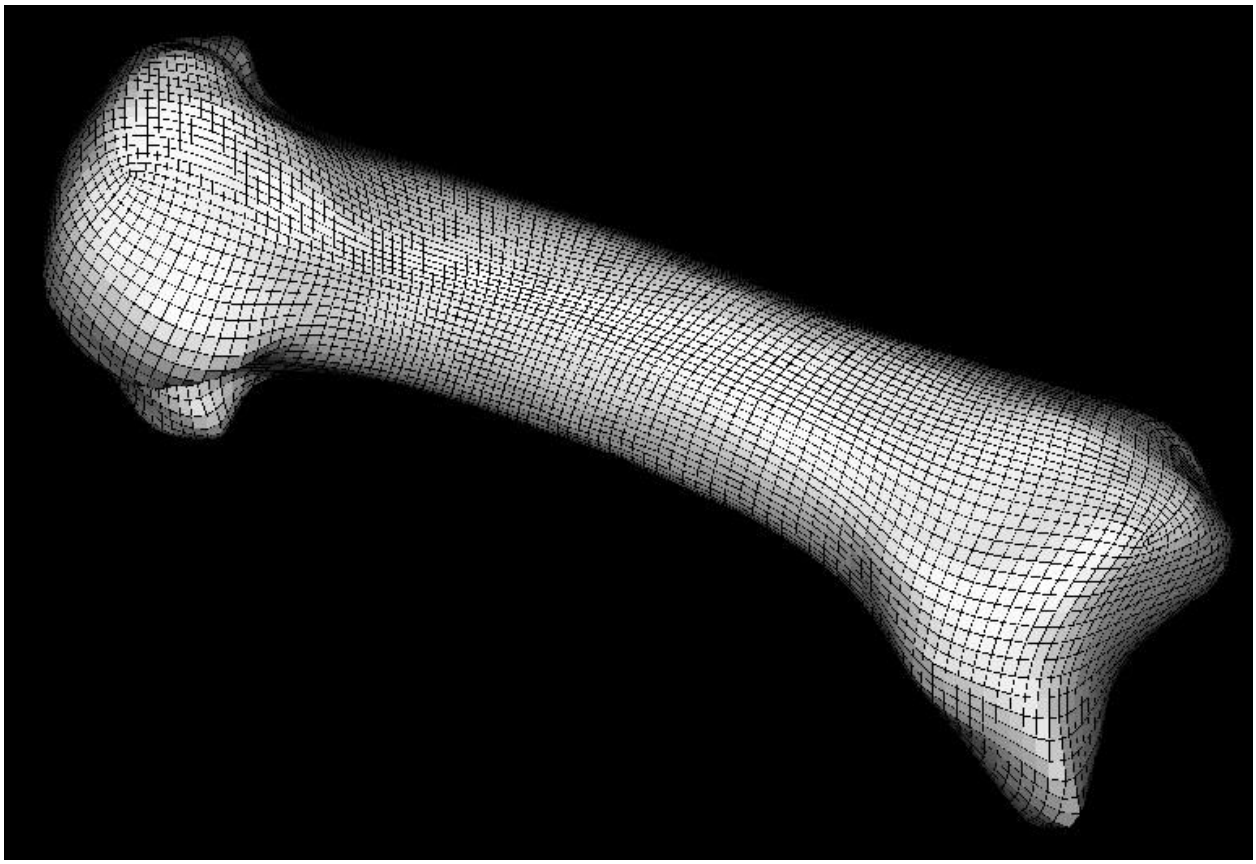

Appendix B: Surface, Block, and Mesh of the Radial and Ulnar Sesamoid

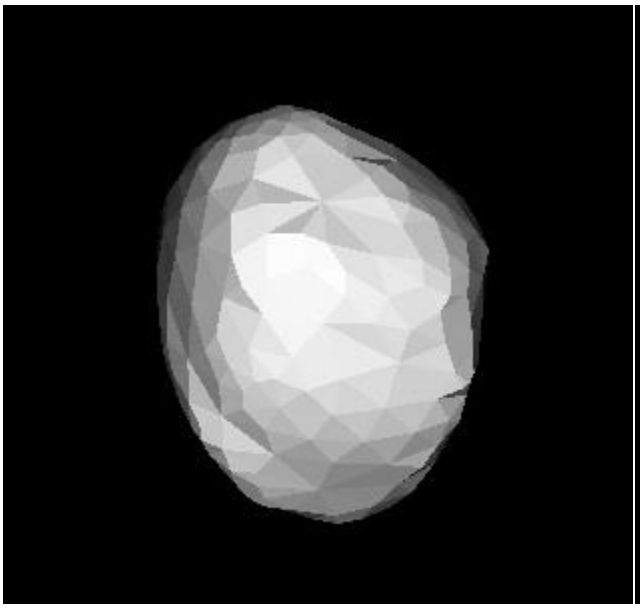

Radial Sesamoid Surface

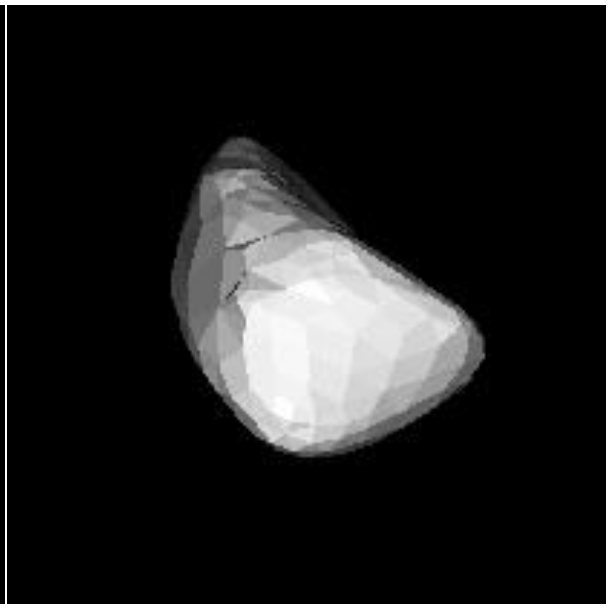

Ulnar Sesamoid Surface

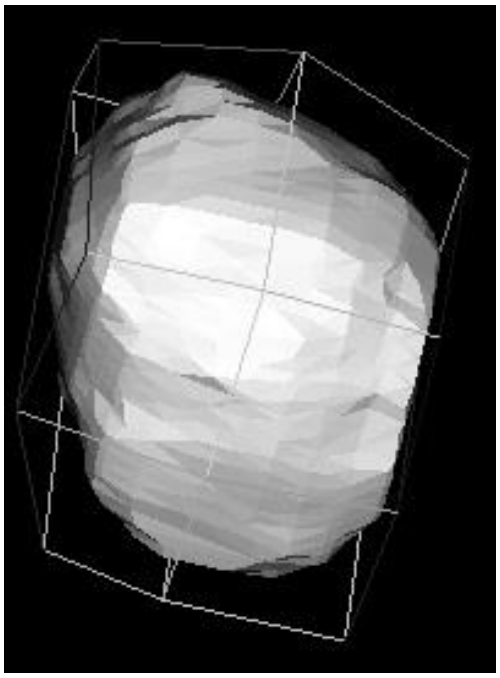

Radial Sesamoid Block

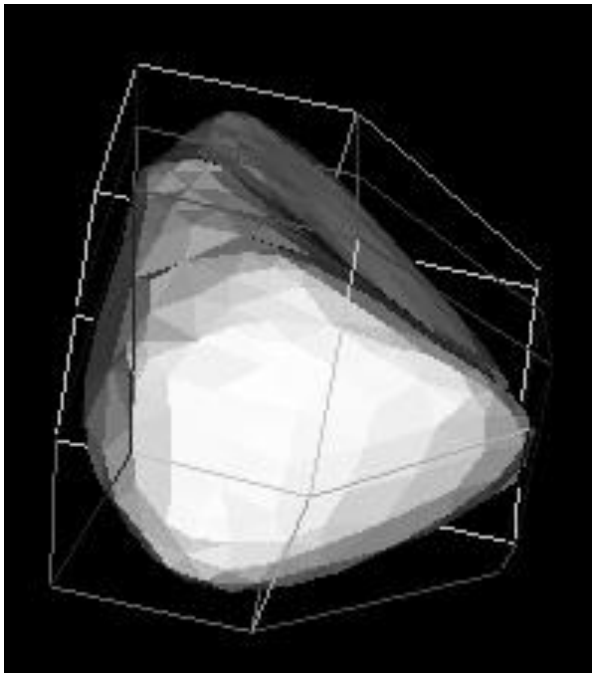

Ulnar Sesamoid Block

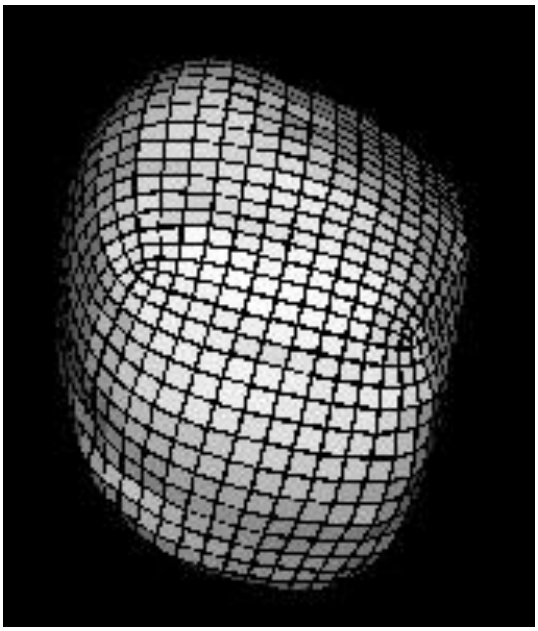

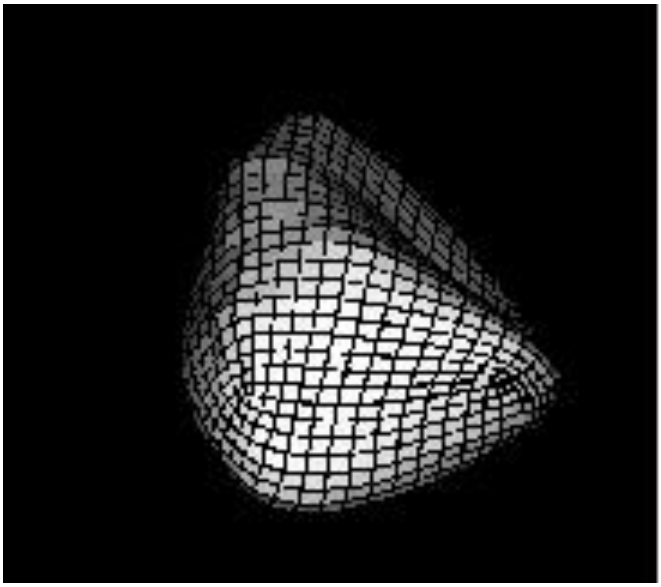

Ulnar Sesamoid Mesh

Appendix D: Thumb Protector, US Patent 5,063,613 (Brown)

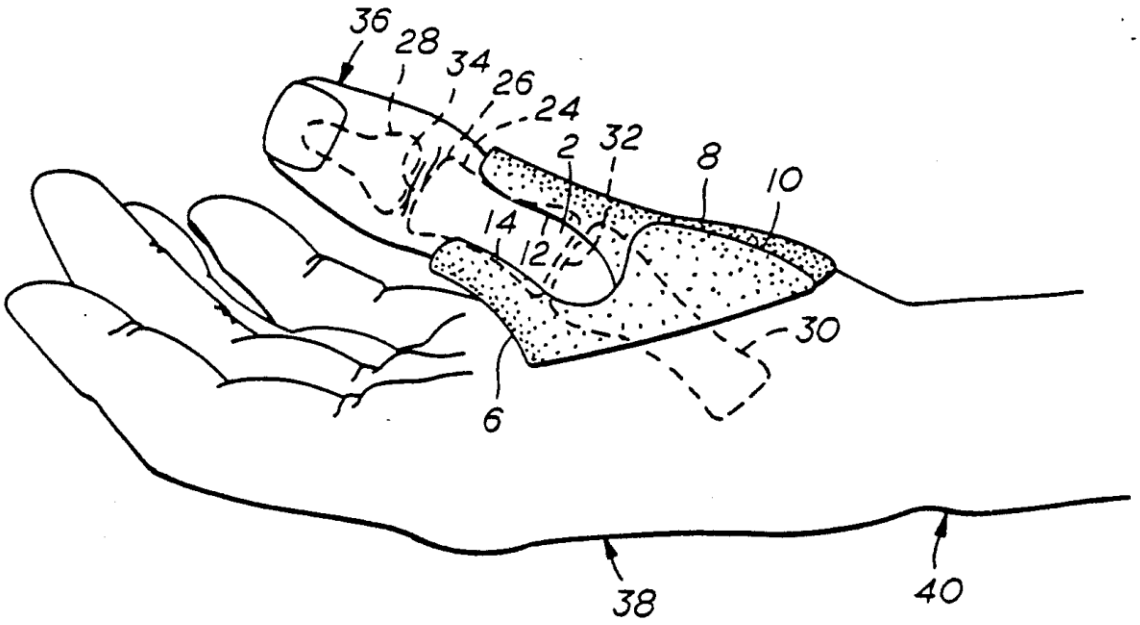

Appendix E: Safety Glove with Modified Dorsal Thumb Spica, US Patent 4,524,464, (Primiano)

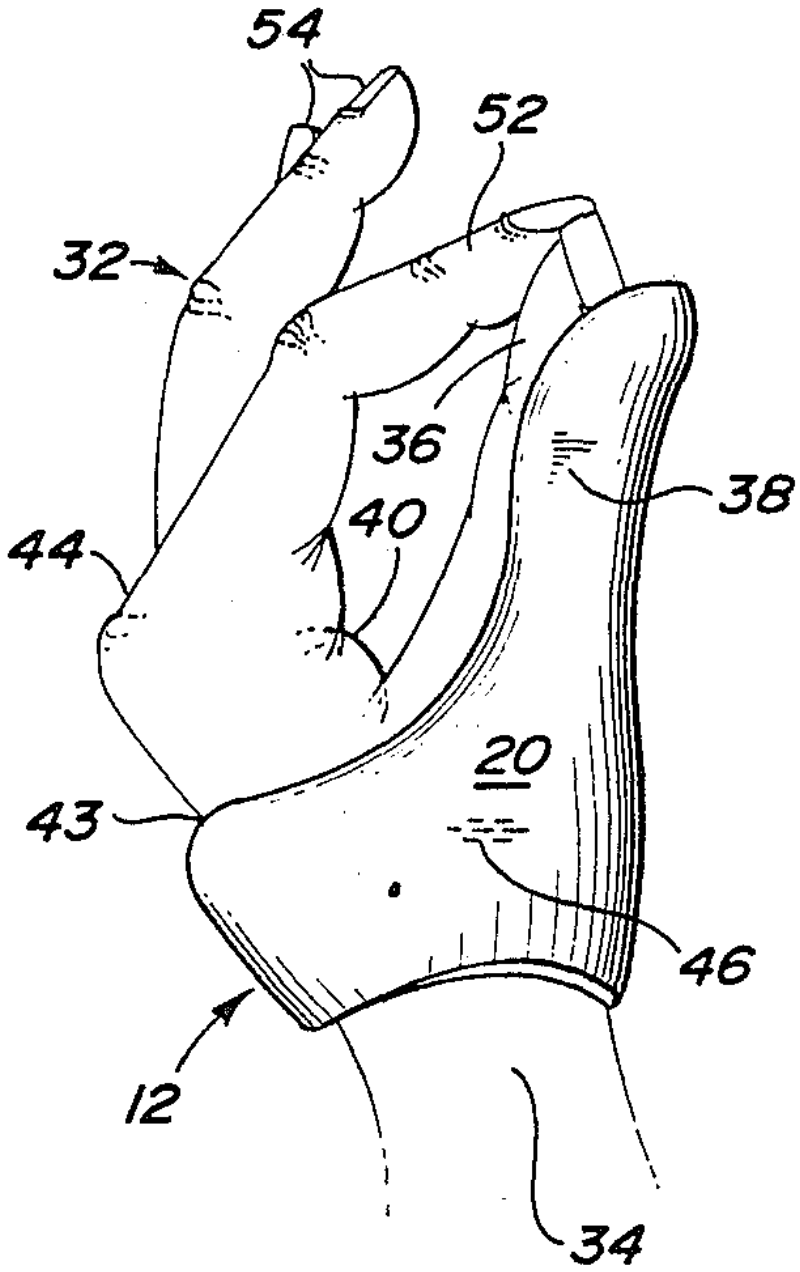

Appendix F: Soccer Glove, European Patent 2,289,359 (Avis)

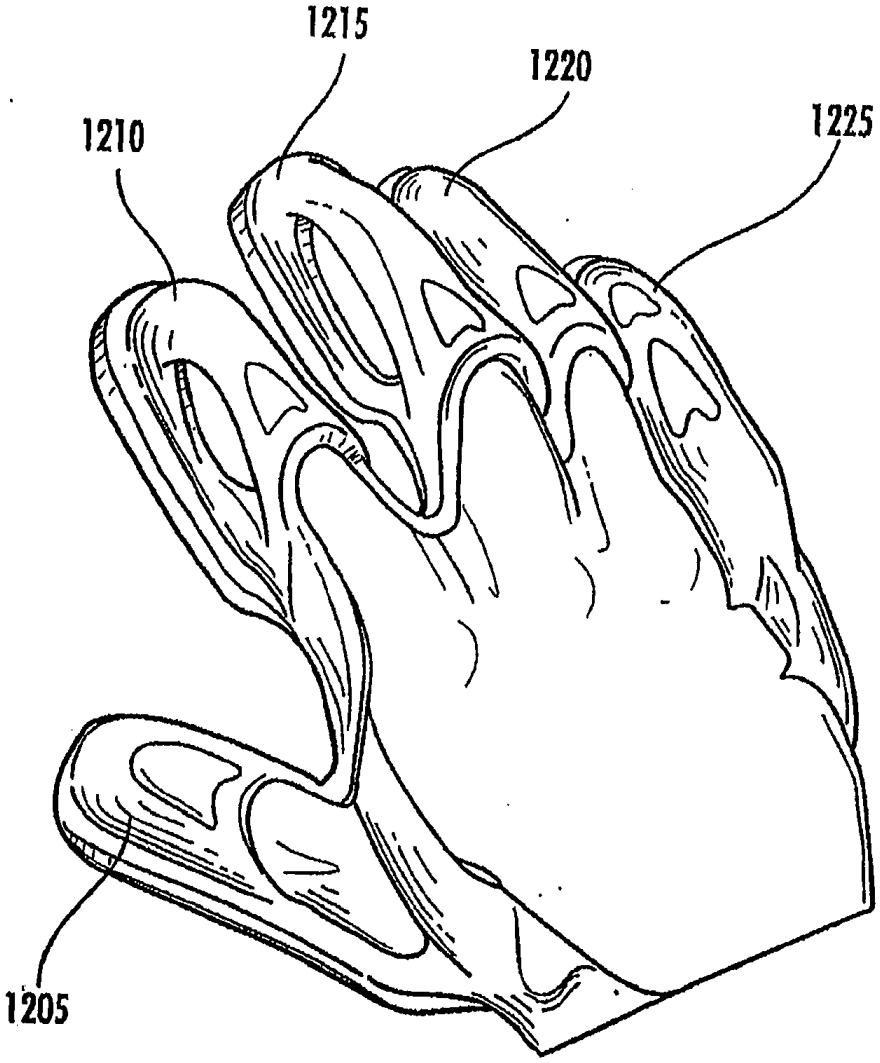

FIG. 12

Appendix G: Goalkeeper's Glove with a Gusset, US Patent 6,654,965 (Hochmuth)

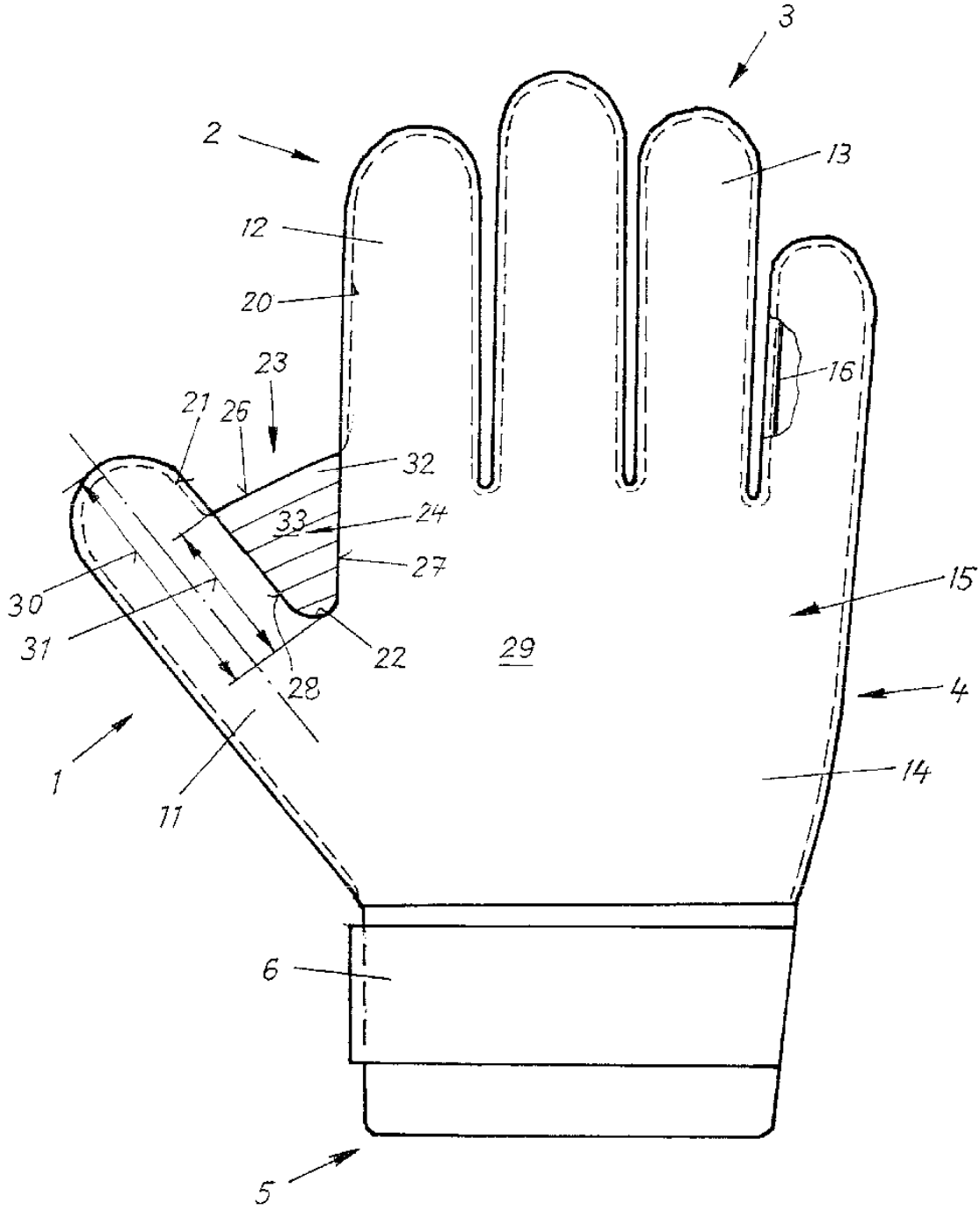

Appendix H: Glove with Support System, US Patent 7,958,568, (Fisher)

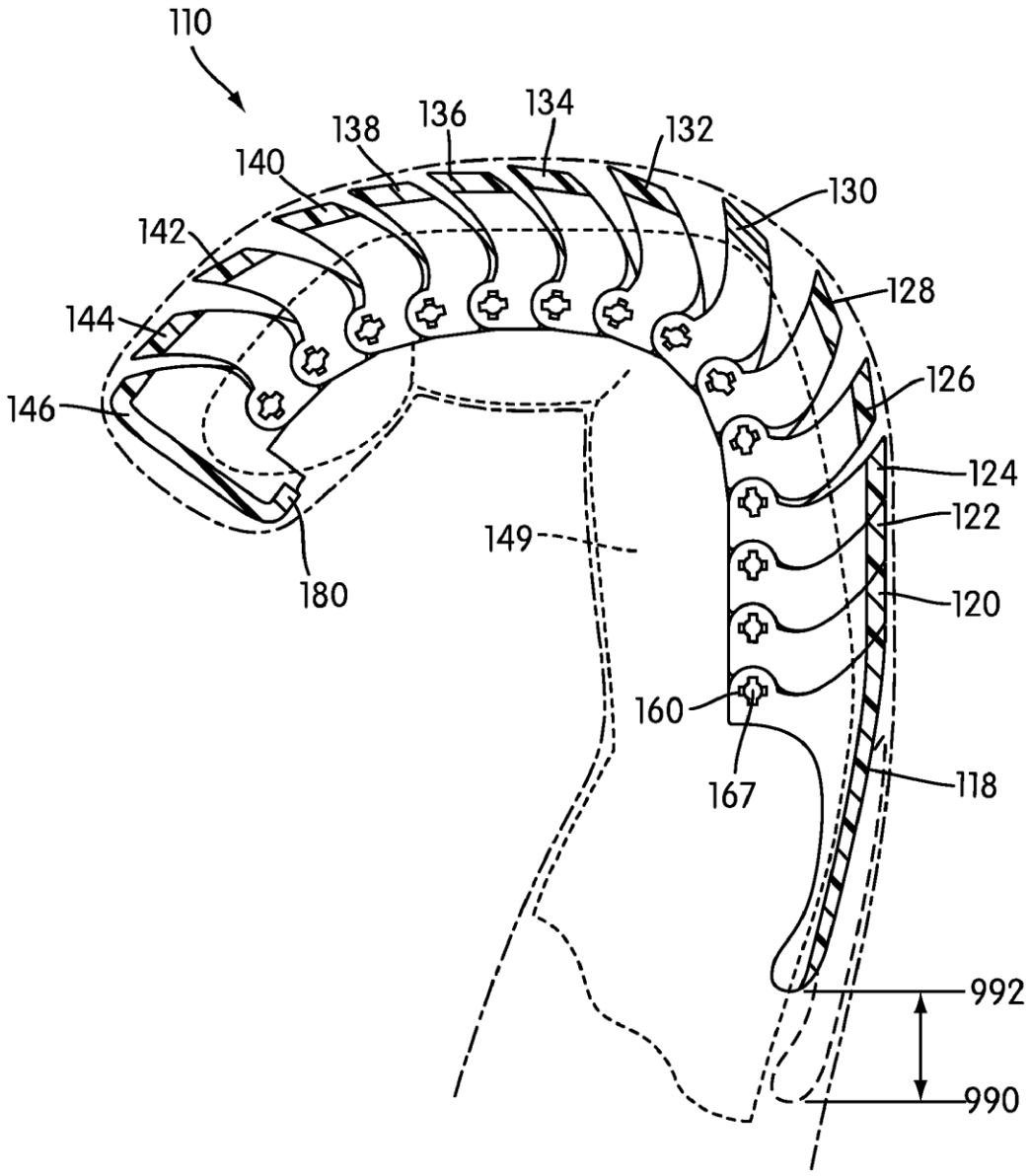

FIG. 20

Appendix I: Objectives Tree

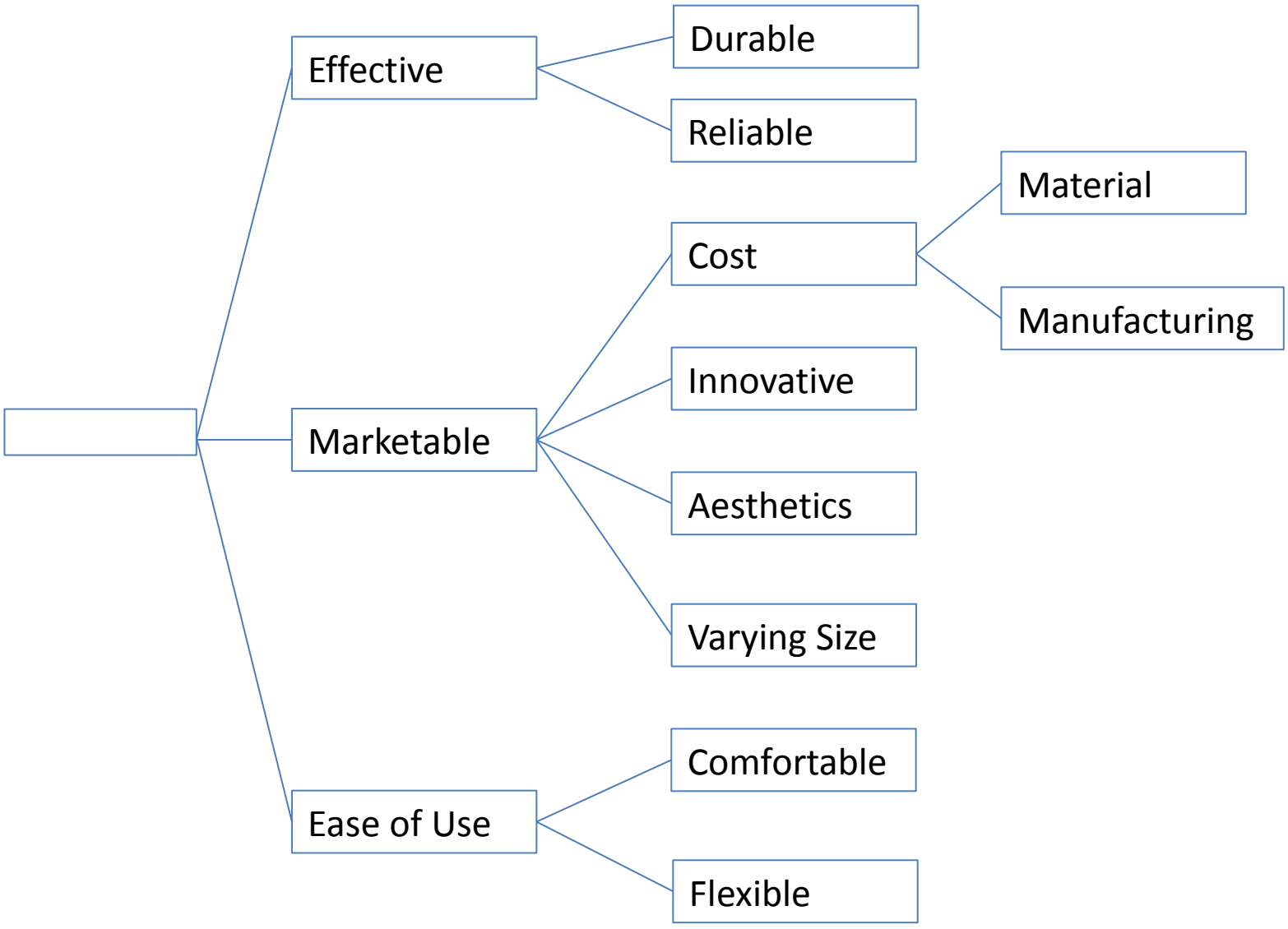

Appendix J: Pairwise Comparison Chart

	Effective	Marketable	Cost	Ease of use	Durable	Aesthetic	Safety	**Total**
Effective		1	1	1	1	1	0.5	**5.5**
Marketable	0		1	0	0	1	0	**2**
Cost	0	0		0	0	1	0	**1**
Ease of use	0	1	1		1	1	0	**4**
Durable	0	1	1	0		1	0	**3**
Aesthetic	0	0	0	0	0		0	**0**
Safety	0.5	1	1	1	1	1		**5.5**

Appendix K: Soft Tissue

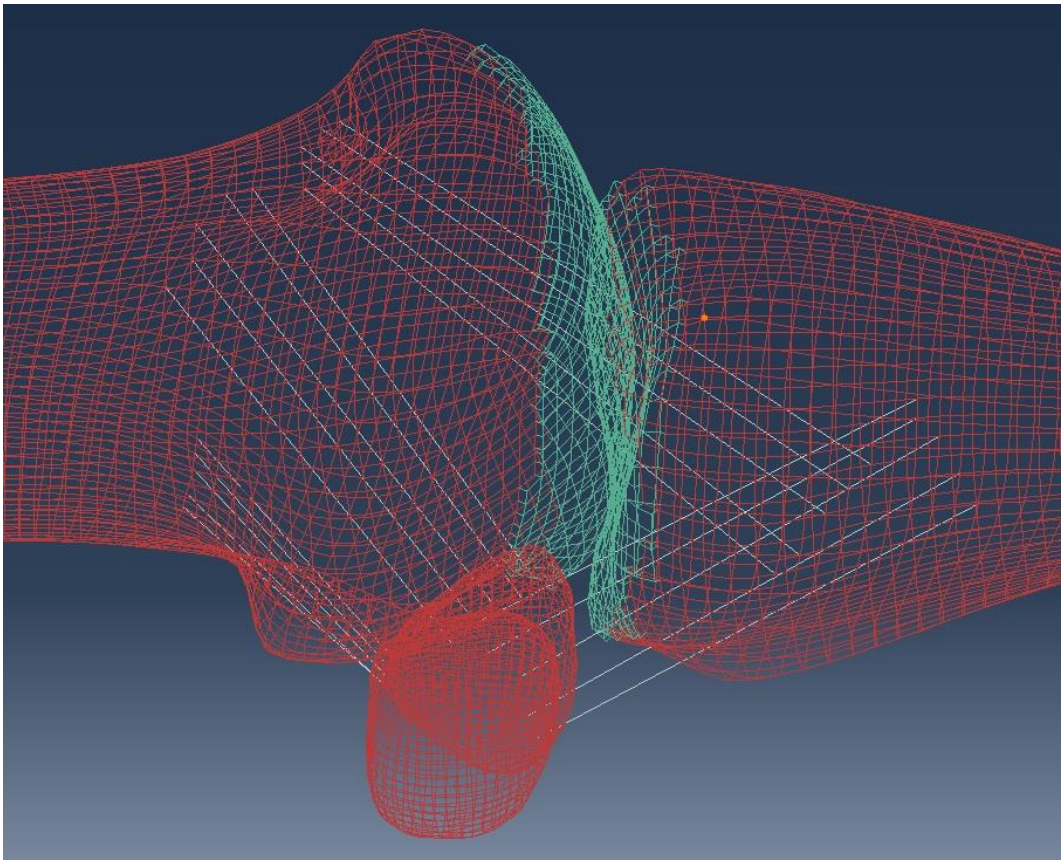

Ulnar Ligaments

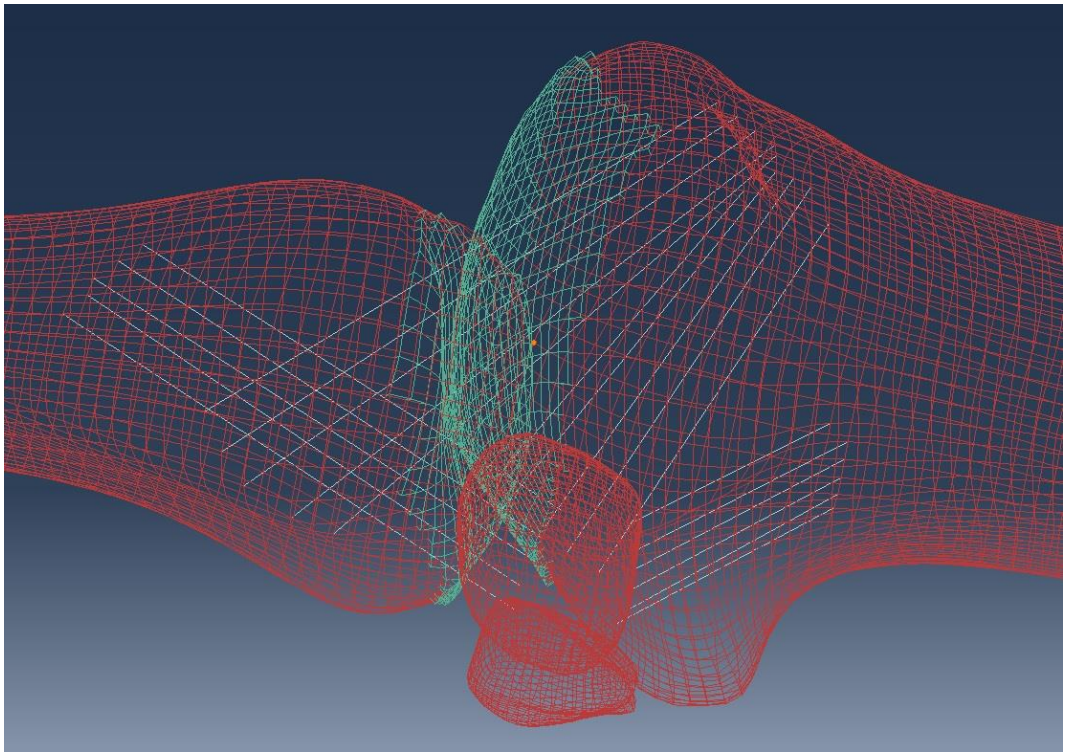

Radial Ligaments

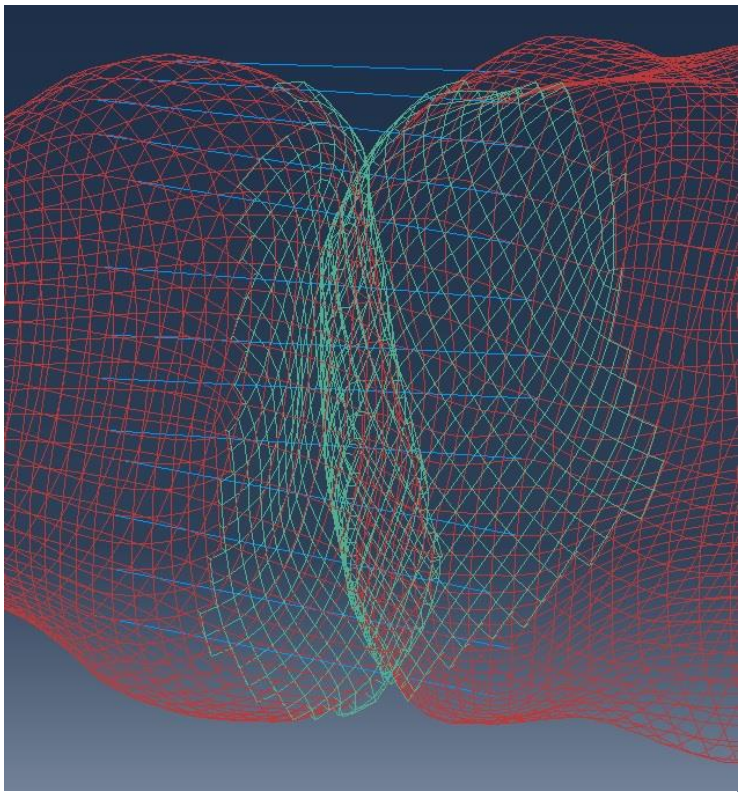

Palmar Plate

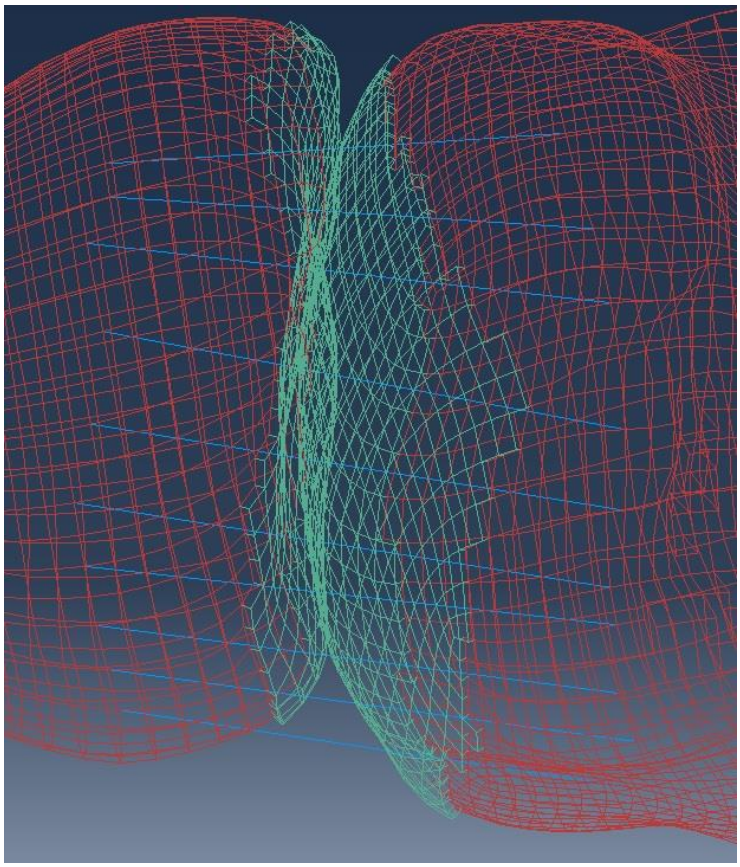

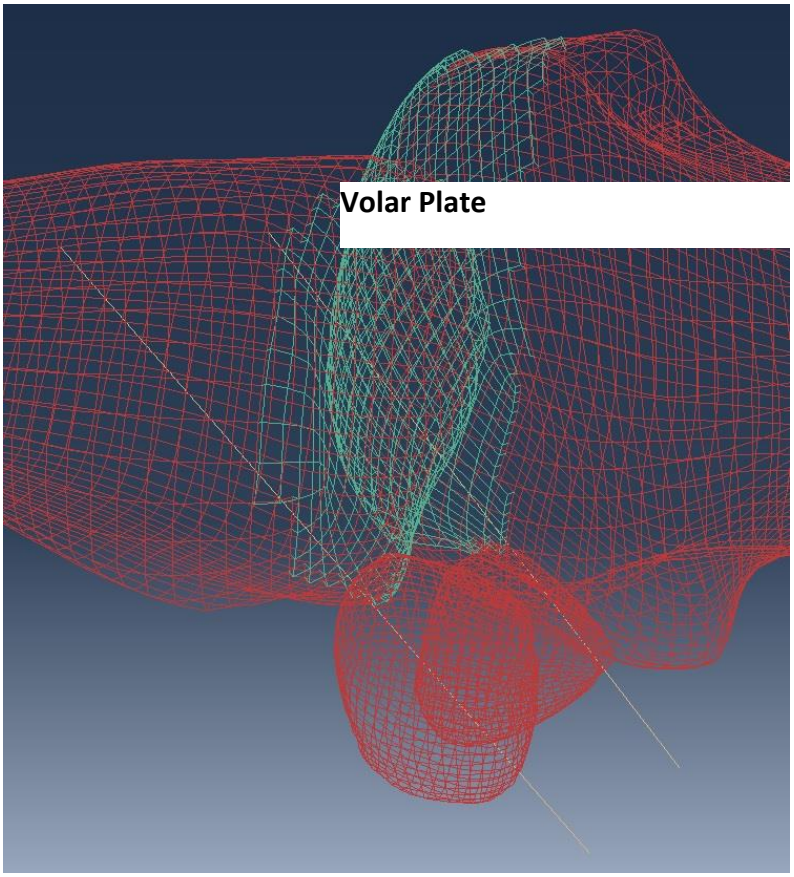

Tendons

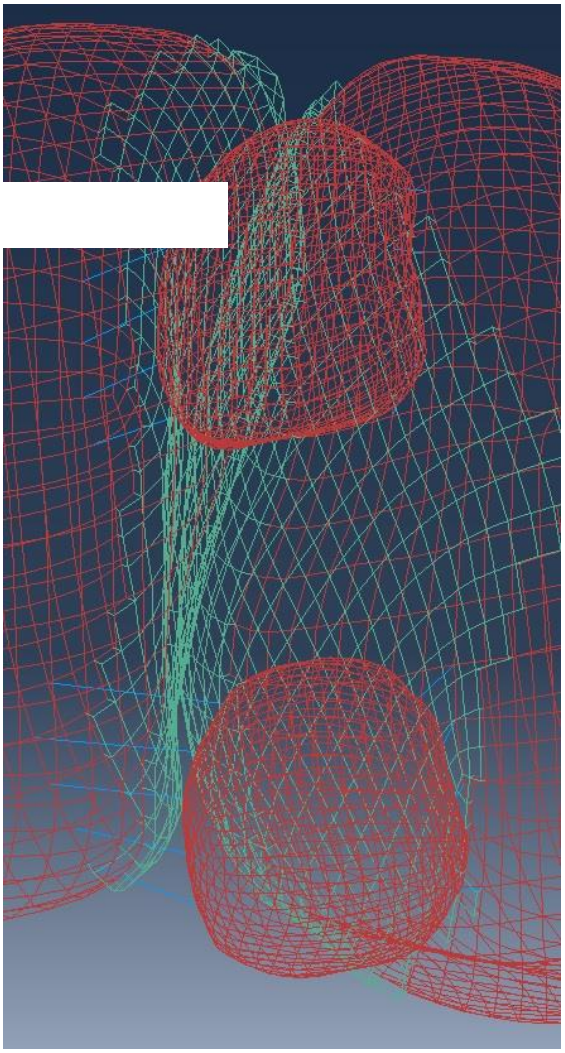

Sesamoid Capsule